

SISSA 77/2004/EP
hep-ph/0410283

High Precision Measurements of θ_\odot in Solar and Reactor Neutrino Experiments

Abhijit Bandyopadhyay¹, Sandhya Choubey^{2,3}, Srubabati Goswami⁴, S.T. Petcov^{3,2,5}

¹ *Theory Group, Saha Institute of Nuclear Physics, 1/AF, Bidhannagar, Calcutta 700 064, India*

² *INFN, Sezione di Trieste, Trieste, Italy.*

³ *Scuola Internazionale Superiore di Studi Avanzati, I-34014 Trieste, Italy.*

⁴ *Harish-Chandra Research Institute, Chhatnag Road, Jhusi, Allahabad 211 019, India.*

⁵ *Institute of Nuclear Research and Nuclear Energy, Bulgarian Academy of Sciences, 1784 Sofia, Bulgaria.*

Abstract

We discuss the possibilities of high precision measurement of the solar neutrino mixing angle $\theta_\odot \equiv \theta_{12}$ in solar and reactor neutrino experiments. The improvements in the determination of $\sin^2 \theta_{12}$, which can be achieved with the expected increase of statistics and reduction of systematic errors in the currently operating solar and KamLAND experiments, are summarised. The potential of LowNu $\nu - e$ elastic scattering experiment, designed to measure the pp solar neutrino flux for high precision determination of $\sin^2 \theta_{12}$, is investigated in detail. The accuracy in the measurement of $\sin^2 \theta_{12}$, which can be achieved in a reactor experiment with a baseline $L \sim 60$ km, corresponding to a Survival Probability MINimum (SPMIN), is thoroughly studied. We include the effect of the uncertainty in the value of $\sin^2 \theta_{13}$ in the analyses. A LowNu measurement of the pp neutrino flux with a 1% error would allow to determine $\sin^2 \theta_{12}$ with an error of 14% (17%) at 3σ from a two-generation (three-generation) analysis. The same parameter $\sin^2 \theta_{12}$ can be measured with an uncertainty of 2% (6%) at 1σ (3σ) in a reactor experiment with $L \sim 60$, statistics of ~ 60 GWkTy and systematic error of 2%. The inclusion of the $\sin^2 \theta_{13}$ uncertainty in the analysis changes the error on $\sin^2 \theta_{12}$ to 3% (9%). The effect of $\sin^2 \theta_{13}$ uncertainty on the $\sin^2 \theta_{12}$ measurement in both type of experiments is considerably smaller than naively expected.

1 Introduction

There has been a remarkable progress in the studies of neutrino oscillations in the last several years. The experiments with solar, atmospheric and reactor neutrinos [1, 2, 3, 4, 5, 6, 7] have provided compelling evidences for the existence of neutrino oscillations driven by non-zero neutrino masses and neutrino mixing. Evidences for oscillations of neutrinos were obtained also in the first long baseline accelerator neutrino experiment K2K [8].

The recent Super-Kamiokande data on the L/E -dependence of multi-GeV μ -like atmospheric neutrino events [6], L and E being the distance traveled by neutrinos and the neutrino energy, and the new more precise spectrum data of KamLAND and K2K experiments [9, 10], are the latest significant contributions to this progress. For the first time the data exhibit directly the effects of the oscillatory dependence on L/E and E of the probabilities of ν -oscillations in vacuum [11]. We begin to “see” the oscillations of neutrinos. As a result of these magnificent developments, the oscillations of solar ν_e , atmospheric ν_μ and $\bar{\nu}_\mu$, accelerator ν_μ (at $L \sim 250$ km) and reactor $\bar{\nu}_e$ (at $L \sim 180$ km), driven by nonzero ν -masses and ν -mixing, can be considered as practically established.

The SK atmospheric neutrino and K2K data are best described in terms of dominant 2-neutrino $\nu_\mu \rightarrow \nu_\tau$ ($\bar{\nu}_\mu \rightarrow \bar{\nu}_\tau$) vacuum oscillations. The best fit values and the 99.73% C.L. allowed ranges of the atmospheric neutrino oscillation parameters $|\Delta m_A^2| = |\Delta m_{31}^2|$ and $\theta_A \equiv \theta_{23}$ read [6]: $|\Delta m_{31}^2| = 2.1 \times 10^{-3}$ eV 2 , $\sin^2 2\theta_{23} = 1.0$, $|\Delta m_{31}^2| = (1.3 - 4.2) \times 10^{-3}$ eV 2 , $\sin^2 2\theta_{23} \geq 0.85$. The sign of Δm_{31}^2 and of $\cos 2\theta_{23}$, if $\sin^2 2\theta_{23} \neq 1.0$, cannot be determined using the existing data.

The combined 2-neutrino oscillation analysis of the solar neutrino and the new KamLAND 766.3 Ty spectrum data shows [9, 12, 13] that the solar neutrino oscillation parameters lie in the low-LMA region : $\Delta m_\odot^2 \equiv \Delta m_{21}^2 = (8.2^{+0.6}_{-0.5}) \times 10^{-5}$ eV 2 , $\tan^2 \theta_\odot \equiv \tan^2 \theta_{12} = (0.40^{+0.09}_{-0.07})$ [9]. The high-LMA solution is excluded at more than 3σ . The value of Δm_{21}^2 is determined with a remarkably high precision of 12% at 3σ . Maximal solar neutrino mixing is ruled out at $\sim 6\sigma$.

The solar and atmospheric neutrino, and KamLAND and K2K neutrino oscillation data require the existence of three-neutrino mixing in the weak charged lepton current. In this case the neutrino mixing is characterised by one additional mixing angle θ_{13} – the only small mixing angle in the PMNS matrix. Three-neutrino analyses of the solar, atmospheric and reactor neutrino data show that $\sin^2 \theta_{13} < 0.05$ [12, 13].

Understanding the origin of the patterns of solar and atmospheric neutrino mixing and of Δm_{21}^2 and Δm_{31}^2 , suggested by the data, is one of the central problems in neutrino physics today. A prerequisite for any progress in our understanding of neutrino mixing is the knowledge of the precise values of solar and atmospheric neutrino oscillation parameters, θ_{12} , Δm_{21}^2 , and θ_{23} , Δm_{31}^2 and of θ_{13} .

In the present article we discuss the possibilities of high precision measurement of the solar neutrino mixing angle θ_{12} in solar and reactor neutrino experiments.

The solar neutrino mixing parameter $\sin^2 \theta_{12}$ is determined by the current KamLAND and solar neutrino data with a relatively large uncertainty of 24% at 3σ . In the future, more precise spectrum data from the KamLAND experiment can lead to even more accurate determination of the value of Δm_{21}^2 . However, these data will not provide a considerably more precise measurement of $\sin^2 \theta_{12}$ owing to the fact that the KamLAND detector is effectively situated at a Survival Probability

MAXimum (SPMAX) [14, 15]. The analysis of the global solar neutrino data taking into account a possible reduction of the errors in the data from the phase-III of the SNO experiment ¹, shows that the uncertainty in the value of $\sin^2 \theta_{12}$ would still remain well above 15% at 3σ [32].

We begin by summarising the results on $\sin^2 \theta_{12}$, obtained using the current global solar and reactor neutrino oscillation data (section 2). We consider the improvements in the determination of $\sin^2 \theta_{12}$, which can be achieved with the expected increase of statistics and reduction of systematic errors in the experiments which are currently operating. In particular, the effect of statistics of 3 kTy of KamLAND data as well as of the data of phase-III of SNO experiment are analysed.

We turn next to future experiments. We discuss first (in Section 3) the possibility of high precision determination of $\sin^2 \theta_{12}$ in a LowNu solar neutrino experiment, designed to measure the sub-MeV components of the solar neutrino flux: pp , pep , CNO , 7Be [16, 17, 18, 19]. It is usually suggested that the LowNu experiments can provide one of the most precise measurements of the solar neutrino mixing angle. Here we perform a detailed quantitative analysis of the precision with which $\sin^2 \theta_{12}$ can be determined in such an experiment. We consider a generic $\nu - e$ scattering experiment measuring the pp neutrino flux. We examine the effect of including representative values of pp neutrino induced electron scattering rates in the χ^2 analysis of the global solar neutrino data. Three values (0.68, 0.72, 0.77) of the rates from the currently allowed 3σ range are considered. The error in the measured rate is varied from 1% to 5%. We evaluate how much the accuracy on $\sin^2 \theta_{12}$ improves by adding the pp flux data in the analysis. The dependence of the $\sin^2 \theta_{12}$ sensitivity on the central value of the measured pp flux as well as on the measurement errors is studied. We compare the precision in $\sin^2 \theta_{12}$ expected with the data on pp neutrinos with the projected $\sin^2 \theta_{12}$ sensitivity achieved using the results from phase-III of SNO experiment and 3 kTy KamLAND data, and comment on the minimum error required in the pp LowNu experiments to improve the precision on $\sin^2 \theta_{12}$. The impact of the uncertainty due to θ_{13} on the allowed ranges of $\sin^2 \theta_{12}$ is studied as well.

We analyse in detail the possibility of a high precision determination of $\sin^2 \theta_{12}$ in a reactor experiment with a baseline $L \sim 60$ km, corresponding to a Survival Probability MINimum (SP-MIN) [14] (Section 4). We investigate the dependence of the precision on $\sin^2 \theta_{12}$ which can be achieved in such an experiment on the baseline, statistics and systematic error. More specifically, the spectrum data is simulated for four different true values of Δm_{21}^2 and the optimal baseline which would give the best measurement of $\sin^2 \theta_{12}$ is determined. Precise knowledge of Δm_{21}^2 allows $\sin^2 \theta_{12}$ to be determined with the highest precision over a relatively wider range of baselines. The effect of $\sin^2 \theta_{13}$ uncertainty on the $\sin^2 \theta_{12}$ determination is investigated in great detail.

The results of the present study are summarised in section 5.

2 Bounds from existing experiments

In this section we review the bounds on Δm_{21}^2 and $\sin^2 \theta_{12}$ from the present solar neutrino and KamLAND reactor neutrino data. We also discuss the projected future bounds that we expect to achieve from the current set of experiments.

¹During this phase the neutral current (NC) rate will be measured in SNO with 3He proportional counters.

2.1 Bounds from current solar and reactor data

For the solar neutrino sector we include the data from

- the radiochemical experiments, Cl [1] and Ga (Gallex, SAGE and GNO combined) [2],
- the 1496 day 44 bin Zenith angle spectrum data from SK [3],
- the 34 bin combined CC, NC and Electron Scattering (ES) energy spectrum data from the phase I (pure D_2O phase) of SNO [4]
- the data on CC, NC and ES total observed rates from the phase II (salt phase) of the SNO experiment [5].

The 8B flux normalisation factor f_B is left to vary freely in the analysis, while for the pp , pep , 7Be , CNO , and hep fluxes we use the predictions and uncertainties from the recent standard solar model (SSM) of BP04 [20]. We skip the details of the χ^2 analysis here which can be found in our earlier papers [21, 22, 23].

We include the 766.3 Ty KamLAND data in our global analysis. For treatment of the latest KamLAND data in our combined analysis we refer the reader to [12], while for the future projected analysis with simulated KamLAND data we refer the reader to [24]. The best-fit from the combined analysis of solar and KamLAND data comes at [12]

- $\Delta m_{21}^2 = 8.4 \times 10^{-5}$ eV 2 , $\sin^2 \theta_{12} = 0.28$, $f_B = 0.88$

In figure 1 we plot $\Delta\chi^2 = \chi^2 - \chi^2_{min}$ as a function of Δm_{21}^2 (right panel) and $\sin^2 \theta_{12}$ (left panel), from a two-generation fit of global solar + KamLAND data. The parameters not shown are allowed to vary freely. From this figure one can easily read off the allowed ranges of the displayed parameter at various confidence levels. The horizontal line for instance shows the 3σ limit corresponding to $\Delta\chi^2 = 9$ for a 1 parameter fit. In Table 1 we present the current 3σ allowed ranges of Δm_{21}^2 and $\sin^2 \theta_{12}$ obtained from the Figure 1. We also show the spread in these parameters which is defined as

$$\text{spread} = \frac{\text{prm}_{max} - \text{prm}_{min}}{\text{prm}_{max} + \text{prm}_{min}} \times 100 \quad (1)$$

where prm is either Δm_{21}^2 or $\sin^2 \theta_{12}$. The Table and the plot demonstrate clearly that KamLAND is extremely sensitive to Δm_{21}^2 . Introduction of KamLAND data with increased statistics progressively reduce the spread in Δm_{21}^2 and with the latest data the 3σ spread is $\sim 12\%$, demonstrating the extraordinary precision that has already been achieved in Δm_{21}^2 . On the other hand, the spread in $\sin^2 \theta_{12}$ is seen to be driven mainly by the solar neutrino data and does not show any marked improvement with the inclusion of the KamLAND data into the analysis. The global data from solar and KamLAND restrict $\sin^2 \theta_{12}$ to 24% at 3σ .

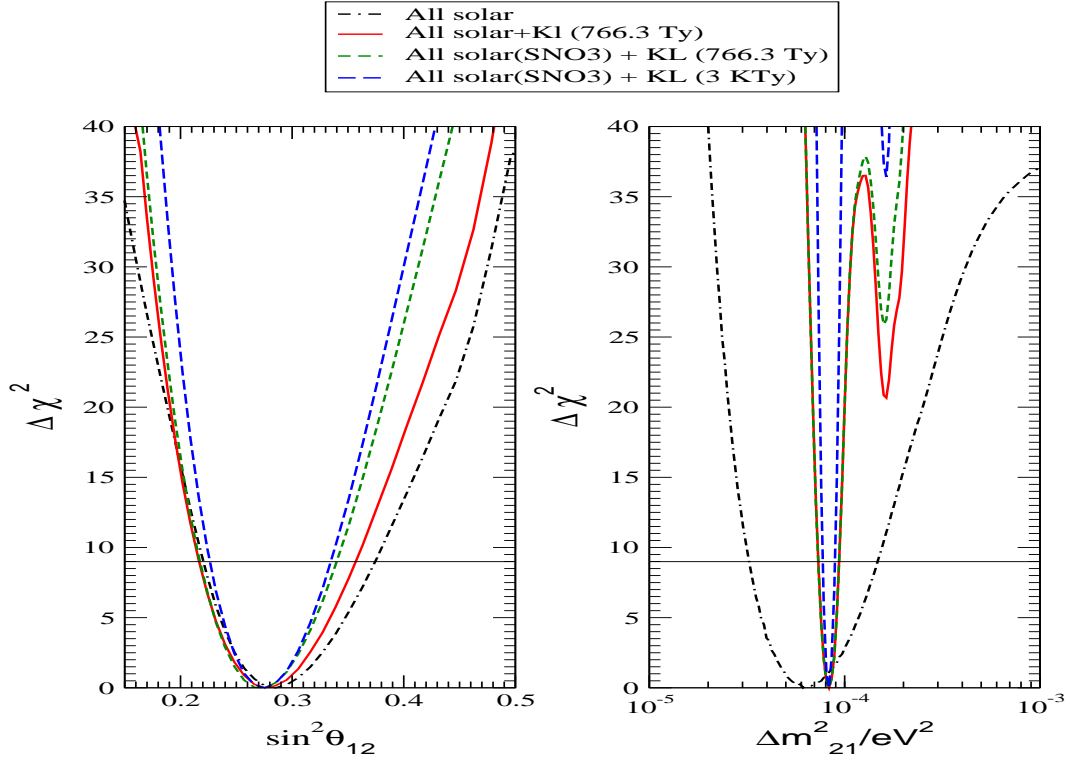


Figure 1: $\Delta\chi^2$ plotted against $\sin^2\theta_{12}$ in left panel and Δm_{21}^2 in right panel. We show the curves obtained from global analysis of current solar neutrino data (black dot-dashed line), current solar + KamLAND data (red solid line), solar neutrino data with projected SNO-III errors + current KamLAND data (green short dashed line) and the solar neutrino data with projected SNO-III errors + projected 3 kTy KamLAND data (blue long dashed line). The horizontal lines display the 3σ limit ($\Delta\chi^2 = 9$) for 1 parameter fit.

2.2 Bounds from prospective data from KamLAND and SNO experiments

Apart from the bounds obtained from the existing data we also present the projected future bounds on Δm_{21}^2 and $\sin^2\theta_{12}$ from the current experiments. In particular, we will discuss the expected impact of future data from KamLAND and SNO experiments on the uncertainty of $\sin^2\theta_{12}$. SNO is sensitive to the 8B neutrinos for which the survival probability for the oscillation parameters in LMA region is the MSW adiabatic probability

$$P_{ee}({}^8B) \approx \sin^2\theta_{12} . \quad (2)$$

The CC/NC ratio in SNO can measure P_{ee} independent of the 8B flux normalisation factor and can thus give a direct measure of the mixing angle $\sin^2\theta_{12}$. Therefore, reducing the error in CC

and NC measurements in SNO can improve the precision of this parameter since

$$\Delta(\sin^2 \theta_{12}) = \Delta(R_{CC}/R_{NC}). \quad (3)$$

KamLAND on the other hand is not sensitive to matter effects and the survival probability is

$$P_{\bar{e}\bar{e}}^{KL} \approx 1 - \sin^2 2\theta_{12} \sin^2 \left(\frac{\Delta m_{21}^2 L}{4E} \right). \quad (4)$$

The average energy and distance in KamLAND corresponds to $\sin^2(\Delta m_{21}^2 L/4E) \approx 0$ i.e it is situated close to a Survival Probability MAXimum (SPMAX). This means that the coefficient of the $\sin^2 2\theta_{12}$ term in $P_{\bar{e}\bar{e}}^{KL}$ is relatively small, weakening the sensitivity of KamLAND to θ_{12} . It can be shown that for the current estimate of its true value, the best measurement of $\sin^2 \theta_{12}$ can be done in a reactor experiment whose baseline is tuned to $\sin^2(\Delta m_{21}^2 L/4E) \approx 1$ i.e it is situated close to a Survival Probability MINimum (SPMIN) [14]. We discuss the results for this experiment in section 4. In this section we present projected results for KamLAND and SNO.

In the phase-III of the SNO experiment, they propose to measure the Neutral Current events through 3He proportional counters. This will help to increase the NC statistics and reduce the NC systematic errors. In addition, the error correlations between CC and NC events will be absent. The total projected error for SNO NC events for this phase is $\sim 6\%$ [25]. We incorporate this in our analysis instead of the present NC error of 9%. For CC events also we assume a reduced total error of 5%. We assume that the central values of the CC and NC rates will remain unchanged. The short dashed lines in Figure 1 display the behavior of $\Delta\chi^2$ for the case where we include the SNO phase-III projected errors with the rest of the solar and 766.3 Ty KamLAND data. The figure shows that with inclusion of SNO phase-III prospective results in our analysis, the allowed range of Δm_{21}^2 in the low-LMA region stays unaltered – being mainly determined by the KamLAND data. However, the higher Δm_{21}^2 regions get more disfavored as the reduced CC and NC errors further disfavor lower values of the 8B flux normalisation. The figure also shows that the allowed range of $\sin^2 \theta_{12}$ gets further constrained on the higher side. From Table 1 we see that the 3σ spread of $\sin^2 \theta_{12}$ becomes 21% with the inclusion of projected SNO phase-III errors in the present set of data.

We also study the effect of increased statistics in KamLAND on the $\sin^2 \theta_{12}$ and Δm_{21}^2 uncertainty. To this end, we include the 3 kTy KamLAND spectrum data simulated at $\Delta m_{21}^2 = 8.3 \times 10^{-5} \text{ eV}^2$, in our analysis with projected SNO phase-III errors. We use a systematic error of 5% for KamLAND since the KamLAND systematics is expected to improve with fiducial volume calibration and re-estimation of nuclear power uncertainties. If the real KamLAND spectral data conforms to this projected spectrum, then the allowed range of Δm_{21}^2 would get further constrained, allowing the determination of Δm_{21}^2 with an accuracy of about 5%. The higher Δm_{21}^2 regions would get further disfavored. The allowed values of $\sin^2 \theta_{12}$ get somewhat more constrained with reduced errors in KamLAND data and the 3σ spread as seen from Table 1 is 18%. Clearly, the $\sin^2 \theta_{12}$ precision cannot be reduced to within 10-15% by the future data from current set of solar and reactor experiments.

Data set used	(3 σ)Range of Δm_{21}^2 eV ²	(3 σ)spread in Δm_{21}^2	(3 σ) Range of $\sin^2 \theta_{12}$	(3 σ) spread in $\sin^2 \theta_{12}$
only sol	3.3 - 15.3	65%	0.22 – 0.38	27%
sol+ 766.3 Ty KL	7.4 - 9.5	12%	0.22 – 0.36	24%
sol(SNO3) + 766.3 Ty KL	7.4 -9.5	12%	0.22 - 0.34	21%
sol(SNO3)+3KTy KL	7.7 -8.9	7%	0.23 - 0.33	18%

Table 1: The 3 σ allowed ranges and % spread of Δm_{21}^2 and $\sin^2 \theta_{12}$ obtained from a 1 parameter fit.

3 Determining θ_{12} from measurement of Solar pp flux

The pp fusion reaction is the main contributor to the observed solar luminosity and the corresponding pp neutrinos constitute the strongest component in the solar neutrino flux. The SSM uncertainty in the predicted solar neutrino fluxes is the least for the pp neutrinos (1%). So far only the Ga experiments have measured the pp neutrino flux because of their low thresholds of 0.23 MeV. Sub-MeV solar neutrino experiments (LowNu experiments) are being planned for detecting the pp neutrinos using either charged current reactions (LENS, MOON, SIREN) or electron scattering process (XMASS, CLEAN, HERON, MUNU, GENIUS) [17, 18, 19]. One of the prime goals of these experiments is to observe the low energy end of the solar neutrino spectrum consisting of the pp , CNO and the 7Be line and do a full solar neutrino spectroscopy. Since in the SSM, most of the energy generation in the Sun is expected to come from the pp reaction, a precise determination of the pp neutrinos would lead to a better understanding of the solar physics. At the same time it has also been realized that high precision measurement of the pp neutrino flux can also be instrumental for more accurate determination of the neutrino mixing parameter, which as we have seen in the earlier section, will not be determined to an accuracy of below 10-15% by the current set of experiments.

Since the pp neutrino energy spectrum extends up to 0.42 MeV only, for Δm_{21}^2 in the LMA region they do not undergo any matter effect either in Sun or in earth. The probability is therefore simply the vacuum oscillation probability with the Δm_{21}^2 term averaged out because of the large distance traveled between earth and sun, and is given as,

$$P_{ee}^{pp} = 1 - \frac{1}{2} \sin^2 2\theta_{12}. \quad (5)$$

The event rate for a $\nu - e$ scattering and charged current experiment measuring pp flux is given respectively as

$$R^{pp} = \langle P_{ee}^{pp} \rangle + r_{pp}(1 - \langle P_{ee}^{pp} \rangle) \text{ for ES experiments,} \quad (6)$$

$$R^{pp} = \langle P_{ee}^{pp} \rangle \text{ for CC experiments,} \quad (7)$$

where $r_{pp} \approx 0.3$. For a charged current experiment the NC contribution represented by the second term is absent. The above gives the uncertainty in $\sin^2 \theta_{12}$ as

$$\Delta(\sin^2 \theta_{12})_{ccpp} \sim \frac{\Delta R^{pp}}{2 \cos 2\theta_{12}} \text{ for CC experiments} \quad (8)$$

$$\Delta(\sin^2 \theta_{12})_{pp} \sim \frac{\Delta R^{pp}}{2 \cos 2\theta_{12}} \frac{1}{1 - r_{pp}} \text{ for ES experiments} \quad (9)$$

A comparison of Eq. (8) with Eq. (3) shows that for the same value of error in the experimentally measured CC pp rate and CC/NC ratio in SNO, the CC pp experiments can give a better accuracy for $\sin^2 \theta_{12}$ only if $\cos 2\theta_{12} > 0.5$ ($\sin^2 \theta_{12} < 0.15$). For the ES pp experiments, because of the presence of about 30% of NC contribution ($r_{pp} \approx 0.3$) in the total ES events, we see by comparing Eq. (9) with Eq. (3) that the ES pp experiment could supersede SNO in measuring $\sin^2 \theta_{12}$ only if the true value of $\cos 2\theta_{12} > 0.71$ ($\sin^2 \theta_{12} < 0.14$). However, since the current allowed 3σ range of $\sin^2 \theta_{12} = 0.22 - 0.38$, we note that in the bulk of the allowed range of $\sin^2 \theta_{12}$, SNO will have a better sensitivity to $\sin^2 \theta_{12}$ for the same experimental error. So it is clear that in order to improve on the measured range of $\sin^2 \theta_{12}$ after the phase-III results from SNO, the total experimental error in the measured event rate in the pp experiments need to be low, which implies high statistics and well understood systematics. Our aim in this section is to quantify the above statements by incorporating hypothetical observed pp rates in our analysis. We consider a generic “pp” ES experiment ² and give quantitative estimate for the $\sin^2 \theta_{12}$ sensitivity expected in these kinds of experiments through projected analyses including global solar and reactor data. We also try to answer the question as to what should be the maximum allowed error in a pp measurement for which the $\sin^2 \theta_{12}$ sensitivity can improve over that expected to be achieved with the SNO phase-III results. We take the predicted pp neutrino flux and its uncertainty from the BP04 SSM. Therefore our analysis includes an 1% error due to SSM uncertainties apart from the experimental errors.

3.1 Two generation analysis

We consider a generic $\nu_e - e$ scattering experiment which is sensitive to the pp neutrinos. We assume a threshold of 50 KeV for the electron K.E. and assume that the Standard Solar Model predicts the pp flux correctly. The predicted rate w.r.t BP04 model, at the current best-fit, for such an experiment is 0.71 while the 3σ range is $0.67 - 0.76$ [12]. We consider three illustrative pp rates of 0.68, 0.72 and 0.77 and vary the experimental error in the pp measurement from 1 to 5%. The theory errors due to SSM and their correlations for the pp fluxes are included in the analysis following the standard covariance approach [26]. Thus we minimise the χ^2 defined as

$$\chi^2_{\odot} = \sum_{i,j=1}^N (R_i^{\text{expt}} - R_i^{\text{theory}})(\sigma_{ij}^2)^{-1}(R_j^{\text{expt}} - R_j^{\text{theory}}) \quad (10)$$

where R_i are the solar data points, N is the number of data points and $(\sigma_{ij}^2)^{-1}$ is the inverse of the covariance matrix, containing the squares of the correlated and uncorrelated experimental and

²A comparison of Eqs. (8) and (9) shows that the CC pp experiments could achieve a better sensitivity on $\sin^2 \theta_{12}$ due to the absence of the $\approx 30\%$ contamination due to NC events present in the ES sample. However, in what follows, we present results for the ES pp experiment keeping the proposed XMASS experiment in mind. Henceforth when we say “pp” experiment we consider an ES pp experiment.

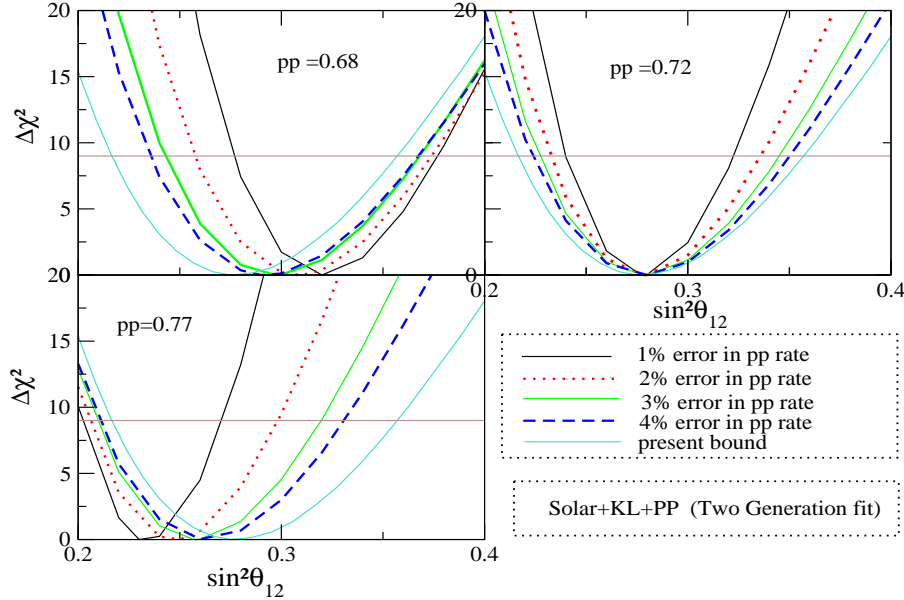


Figure 2: $\Delta\chi^2$ vs. $\sin^2\theta_{12}$ obtained from a two generation analysis of the KamLAND results and the global solar neutrino data including the pp rate. The three panels show the results for the three illustrative values of the pp rate and for each case we present the plots for four different values of the % error in the pp rate. We also show the curve obtained from global analysis of the current solar and reactor data. The horizontal line displays the 3σ limit ($\Delta\chi^2 = 9$) for 1 parameter fit.

theoretical errors. The 8B flux normalisation factor f_B is left to vary freely in the analysis. But the error and correlation due to the other fluxes are taken from the BP04 SSM ³.

Let us begin by analysing first the data from the future pp electron scattering experiments alone. In this case the Eq. (6) can be used to get the approximate values of $\sin^2\theta_{12}$ for a given pp rate,

$$\sin^2 2\theta_{12} \approx \frac{2(1 - R_{pp})}{1 - r_{pp}} \quad (11)$$

where $r_{pp} \approx 0.3$. If we assume a pp rate of 0.72 and consider a 1% experimental error in addition to the SSM error, then the 3σ range of allowed values of $\sin^2\theta_{12}$ from a χ^2 analysis is $0.21 < \sin^2\theta_{12} < 0.33$. This agrees very well from what one would obtain using Eq. (11) including the errors along with the central pp rate of 0.72. This corresponds to a spread of about 22% in $\sin^2\theta_{12}$, which is not much better than what we have from the current data. However, in a realistic scenario, one should analyse the global data on solar neutrinos and not just the pp data alone. In what follows,

³One can also keep the normalisation of the pp neutrino flux as a variable parameter, subject to the luminosity constraint. In such a scenario the astrophysical uncertainties for the pp fluxes need not be taken into account [16].

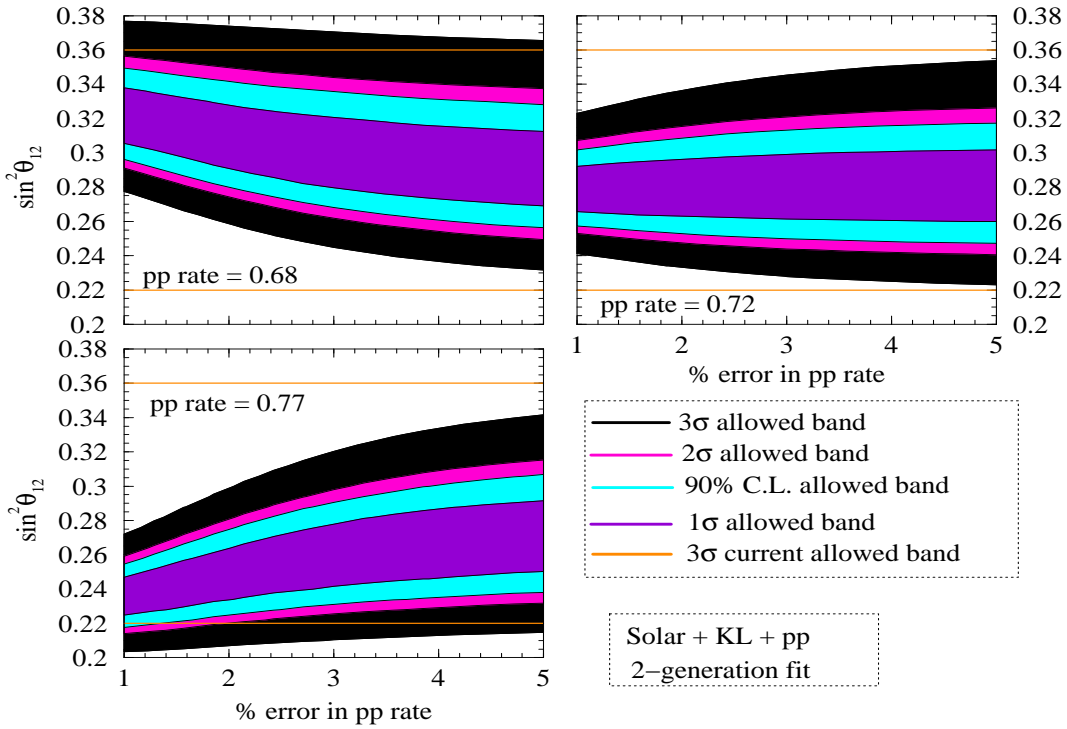


Figure 3: Sensitivity plot showing the 1σ (68.27% C.L.), 1.64σ (90% C.L.), 2σ (95.45% C.L.) and 3σ (99.73% C.L.) allowed range of $\sin^2 \theta_{12}$ as a continuous function of the error in pp rate for three different values of measured pp rate. We also show the current 3σ allowed range of $\sin^2 \theta_{12}$.

we will include the data from all experiments when estimating the sensitivity of the pp rate to the mixing angle θ_{12} .

Figures 2 and 3 show our results for the two-generation analysis of the KamLAND and global solar neutrino data, including the assumed pp measured rates. In Figure 2 we plot the $\Delta\chi^2$ vs $\sin^2 \theta_{12}$ with pp fluxes included in the global χ^2 analysis of solar and KamLAND data. We show the results for measured pp error of 1%, 2%, 3% and 4%. The cyan colored lines show the plots for the current data set. The advantage of having this figure is that one can easily read the range of allowed values of $\sin^2 \theta_{12}$ at any C.L. for a certain experimental error in the pp measurement. In Figure 3 we plot the corresponding allowed range of $\sin^2 \theta_{12}$ from the global analysis of KamLAND and solar data including the LowNu pp rate, as a function of the error in the pp measurement. We let the pp rate error vary from 1% to 5%. The various bands correspond to 68.27% C.L. (1σ), 90% C.L. (1.64σ), 95.45% C.L. (2σ) and 99.73% C.L. (3σ). The horizontal lines on the figure show the current 3σ range of allowed values of $\sin^2 \theta_{12}$ for comparison. In both the figures we present the results for the 3 assumed values of the measured pp rate. The figures show that:

1. For the pp rate of 0.68, which is at the lower end of the range of predicted pp rates, the lower bound on $\sin^2 \theta_{12}$ improves with reduced error in pp flux measurement and the upper bound

worsens. The effect of reducing the error in pp measurement is less on the upper limit.

2. For the pp rate of 0.72 which is close to the best-fit predicted rate, both the lower as well as the upper bounds tighten. Reducing the error in pp flux measurement improves the precision.
3. For the very high pp rate of 0.77, the lower bound on θ_{12} becomes slightly worse while the upper bound becomes better.

These features can be understood by studying the expression for survival probability for pp neutrinos given in Eq. (6). It is evident that a lower pp rate drives $\sin^2 \theta_{12}$ towards higher values and vice versa. Therefore the lower bound on $\sin^2 \theta_{12}$ becomes stronger for pp rate = 0.68. The effect of reducing the error in pp flux measurement improves the lower bound by pushing θ_{12} towards higher values. Likewise we would expect that the upper bound on $\sin^2 \theta_{12}$ should become equally weaker for pp rate = 0.68. However, since we have taken the global solar neutrino data in the analysis, the upper bound on $\sin^2 \theta_{12}$ only gets slightly weakened, as these higher values of $\sin^2 \theta_{12}$ are already severely constrained from the present set of experiments. Thus if a future pp scattering experiment measures a rate near the lower end of the present predicted range the lower limit on $\sin^2 \theta_{12}$ will improve with reduced error in pp rate. The upper limit will weaken slightly but the effect of reducing pp error will not be drastic.

On the other hand, to explain a higher measured pp rate of 0.77, one requires a lower values of $\sin^2 \theta_{12}$. Consequently, the upper limit on $\sin^2 \theta_{12}$ is seen to fall sharply. Even the lower limit on $\sin^2 \theta_{12}$ could be pushed to very low values by the pp experiment alone. However, these values of $\sin^2 \theta_{12}$ are already constrained by the current data set and therefore the lower limit on $\sin^2 \theta_{12}$ cannot reduce much beyond the current allowed range.

A pp rate of 0.72 is quite consistent with the current best-fit parameters and therefore both the upper and lower limits improve with reduced error in pp measurement.

We summarize in Table 2, the range of allowed values of $\sin^2 \theta_{12}$ expected from a combined analysis of KamLAND and current global solar neutrino data and the future data from the pp experiment. With a 1% experimental error in the pp rate, the 3σ spread is about 15%. We note that the range of allowed values of $\sin^2 \theta_{12}$ depends crucially on the measured value of the pp rate. For a measured pp rate of 0.72, which is consistent with the current prediction at the best-fit, both the upper and lower bounds improve. However for pp rate of 0.68 (0.77) only the lower (upper) bound show marked improvement. But note that even though the actual range of allowed values of $\sin^2 \theta_{12}$ depends on the central value of the pp rate, the spread in $\sin^2 \theta_{12}$ is practically independent of the central value of the pp rate. For $R_{pp} = 0.72$, the 3σ $\sin^2 \theta_{12}$ spread is $\approx 23\%$, 19%, 18% and 14% respectively for pp error of 4%, 3%, 2% and 1% as is summarised in Table 2 (4th column). The 3σ spread in $\sin^2 \theta_{12}$ after including the SNO-III data would be about 21%, as in Table 1. If the measured pp rate conforms to a value which is close to the current best-fit predicted pp rate, then the error in pp flux measurement should at least be $\lesssim 3\%$ in order for the pp flux measurement to bring any further improvement in both lower and upper limit of $\sin^2 \theta_{12}$.

In Figure 3 we have included the present solar and KamLAND data and the future pp rates. However we would have the results from the Phase-III of the SNO experiment when the pp experiments start operating. In Figure 4 we show the sensitivity of $\sin^2 \theta_{12}$ to reduced error in the measured pp rate, after including the projected errors for SNO3 in the global analysis. If the

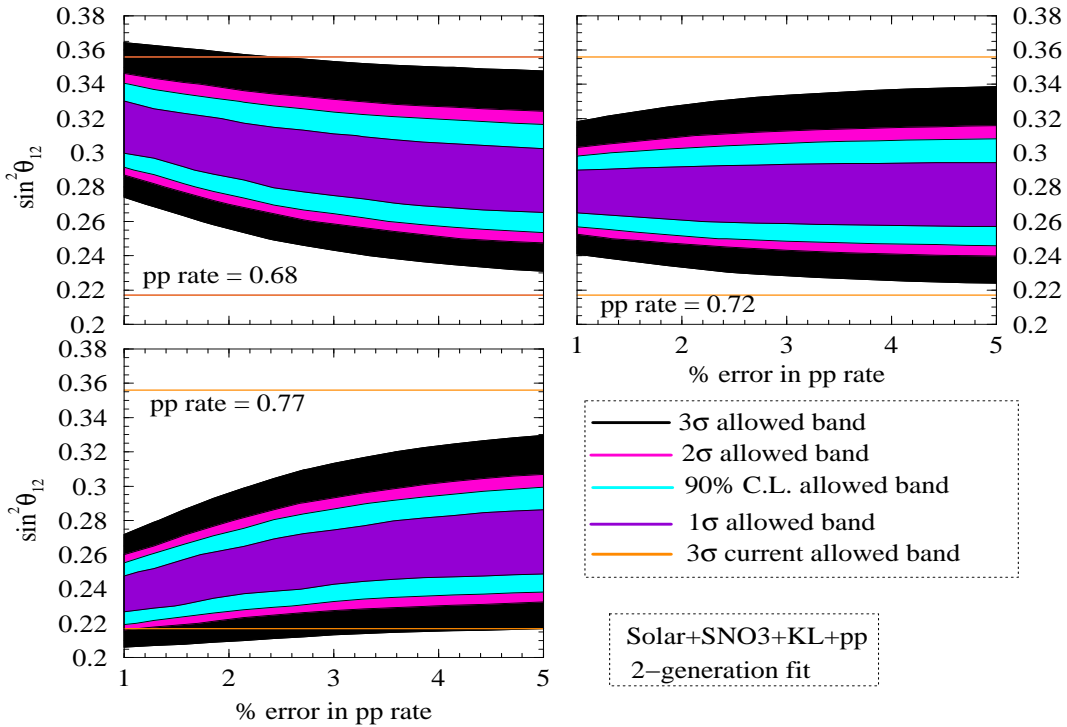


Figure 4: Same as Figure 3 but including the projected error from the third phase of the SNO experiment.

measured pp rate is 0.68(0.77), upper(lower) limit slightly weakens and lower(upper) limit significantly improves, but again the total uncertainty in $\sin^2 \theta_{12}$ is independent of the central value of the pp rate. For $R_{pp} = 0.72$, the 3σ spread in $\sin^2 \theta_{12}$ is $\approx 21\%$, 18% , 18% , 14% respectively for 4%, 3%, 2% and 1% errors. It follows that for all cases one needs a pp error of $\lesssim 4\%$ to have an improvement over the projected uncertainty of 21% in $\sin^2 \theta_{12}$ after SNO phase-III. Table 2 summarises the allowed ranges and spread of $\sin^2 \theta_{12}$ from a two generation analysis including SNO-III projected errors. The spread in $\sin^2 \theta_{12}$ reduce with SNO-III as expected. Note that the ranges given in Table 2 are with the present KamLAND data. If we use increased statistics in KamLAND the allowed spread in $\sin^2 \theta_{12}$ may reduce, albeit slightly.

3.2 Impact of non-zero θ_{13}

One further uncertainty in the precision measurement of $\sin^2 \theta_{12}$ can arise from our lack of knowledge of the precise value of $\sin^2 \theta_{13}$. In this section we explore this aspect. This warrants a three generation analysis and in addition to the solar and KamLAND data, we need to introduce the constraints from atmospheric [6] and CHOOZ experiments [27]. The oscillation parameters for a three flavor analysis are two mass squared differences $\Delta m_{21}^2 = \Delta m_{\odot}^2$, $\Delta m_{31}^2 = \Delta m_{CHOOZ}^2 \simeq \Delta m_{atm}^2 = \Delta m_{32}^2$ and three mixing angles, which are usually denoted as θ_{12} , θ_{23} and θ_{13} with the mixing matrix parameterized in the standard PMNS form. The latest value for the best-fit

pp rate	% error	solar+reactor +pp		solar(SNO3)+reactor+pp	
		3 σ range	spread	3 σ range	spread
0.68	1	0.28 - 0.38	15.2%	0.27 - 0.36	14.3%
	2	0.26 - 0.37	17.5%	0.26 - 0.36	16.1%
	3	0.24 - 0.37	21.3%	0.24 - 0.35	18.6%
	4	0.24 - 0.37	21.3%	0.23 - 0.35	20.6%
0.72	1	0.24 - 0.32	14.3%	0.24 - 0.32	14.3%
	2	0.23 - 0.33	17.9%	0.23 - 0.33	17.9 %
	3	0.23 - 0.34	19.3%	0.23 - 0.33	17.9 %
	4	0.22 - 0.35	22.8%	0.22 - 0.34	21.4%
0.77	1	0.20 - 0.27	14.9%	0.20 - 0.27	14.9%
	2	0.21 - 0.30	17.6%	0.21 - 0.30	17.6%
	3	0.21 - 0.32	20.8%	0.21 - 0.31	19.2%
	4	0.21 - 0.33	22.2%	0.21 - 0.32	20.8%

Table 2: The 3σ allowed ranges and % spread of $\sin^2 \theta_{12}$ obtained from a two generation analysis of the solar neutrino data including the pp rate and KamLAND data.

Δm_{atm}^2 from the two generation analysis of the zenith-angle SK data is 2.1×10^{-3} eV 2 [6]. Therefore independent two generation oscillation analyses of atmospheric and solar neutrino data indicate $\Delta m_{21}^2 \ll \Delta m_{32}^2$. In this limit the three generation neutrino/antineutrino survival probability for solar and KamLAND is given by the following expression:

$$P_{ee}^{3gen} \cong \cos^4 \theta_{13} P_{ee}^{2gen} + \sin^4 \theta_{13} \quad (12)$$

where P_{ee}^{2gen} is the ν_e survival probability for two-neutrino mixing (see, e.g., [28]). For KamLAND the two-generation probability is given by Eq. (4). In the case of solar neutrinos, $P_{ee}^{2gen} \equiv P_{ee\odot}^{2gen}$ is the two-neutrino oscillation ν_e survival probability [29] with the solar electron number density N_e replaced by $N_e \cos^2 \theta_{13}$. Therefore

$$P_{ee}(^8B)^{3gen} \cong \cos^4 \theta_{13} \sin^2 \theta_{12}, \quad (13)$$

$$P_{ee}(pp)^{3gen} \cong \cos^4 \theta_{13} (1 - \frac{1}{2} \sin^2 2\theta_{12}). \quad (14)$$

Note that for a given value of $P_{ee}(pp)^{3gen}$, a non-zero value of θ_{13} *decreases* the measured value of θ_{12} , for the low energy pp flux. On the other hand, for a given value of $P_{ee}(^8B)^{3gen}$, a non-zero value of θ_{13} *increases* the measured value of θ_{12} , for the higher energy 8B flux.

In the limit $\Delta m_{21}^2 \ll \Delta m_{31}^2$, the probability relevant for CHOOZ is given by

$$P_{ee\text{CHOOZ}}^{3gen} \approx 1 - \sin^2 2\theta_{13} \sin^2(\Delta m_{31}^2 L / 4E). \quad (15)$$

We note that the CHOOZ probability depends on Δm_{31}^2 unlike solar and KamLAND. We allow Δm_{31}^2 to vary freely within the 3σ allowed range given in [6]. The details of our three neutrino analysis can be found in [30].

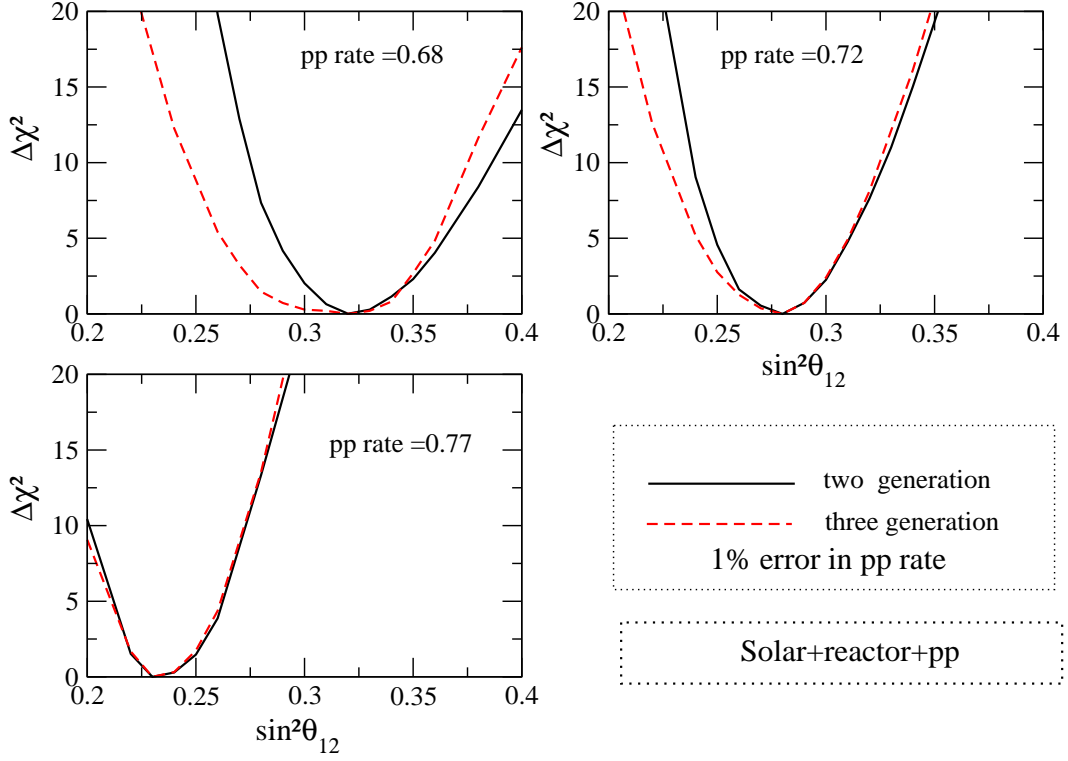


Figure 5: Comparison of $\Delta\chi^2$ vs. $\sin^2\theta_{12}$ obtained from a two generation analysis (solid black line) and three generation analysis (dashed red line) analyses of the world neutrino data including the pp rate. The three panels show the results for the three illustrative values of the pp rate. We present the results for 1% error in the pp rate. For the three generation analysis $\sin^2\theta_{13}$ is allowed to vary freely. and for each case we present the plots for four different values of the % error in the pp rate.

In figure 5 we show the $\Delta\chi^2$ vs $\sin^2\theta_{12}$ obtained for the three generation analysis of the combined KamLAND, CHOOZ and solar neutrino data including the pp rates, where all the other parameters including $\sin^2\theta_{13}$ are allowed to vary freely. For the sake of comparison we also plot the $\sin^2\theta_{13} = 0$ case in the same plot. We make this comparison for the three illustrative central values for the pp rates used earlier, but here we plot the case for 1% error in R_{pp} only. We find that for a lower value of measured pp rate of 0.68, a non-zero $\sin^2\theta_{13}$ weakens both the lower and the upper bounds. For 0.72 the lower bound weakens while the upper bound remains unaffected. For 0.77 both limits are practically unaffected.

To help explain these features, we plot in figure 6 the pp scattering rate (cf. Eqs. (6) and (14)) as a function of $\sin^2\theta_{12}$ for $\sin^2\theta_{13} = 0$ and $\sin^2\theta_{13} = 0.05$, which is the current 3σ upper limit of $\sin^2\theta_{13}$ from our global analysis. We also show three horizontal lines corresponding to the three pp rates considered in our analysis. We see from the figure that,

1. for a given value of $\sin^2\theta_{12}$, a non-zero $\sin^2\theta_{13}$ always reduces the predicted pp rate,

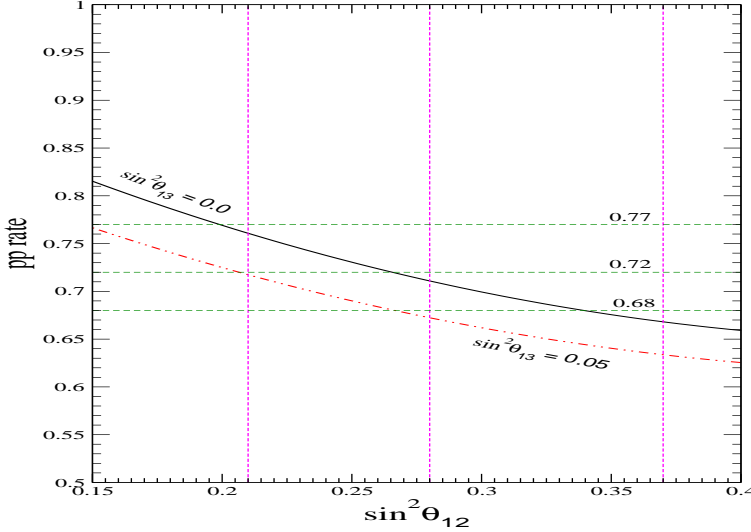


Figure 6: The pp rate as a function of $\sin^2 \theta_{12}$. The black solid line is the pp rate for $\sin^2 \theta_{13} = 0$ while the red dot-dashed line is $\sin^2 \theta_{13} = 0.05$. We also show our illustrative pp rates of 0.68, 0.72 and 0.77 on the plot.

2. for a measured pp rate, a non-zero $\sin^2 \theta_{13}$ would reduce the measured value of $\sin^2 \theta_{12}$,
3. there is always a limiting value of $\sin^2 \theta_{12}$, above which $\sin^2 \theta_{13}$ ceases to make any difference to the bound on $\sin^2 \theta_{12}$ for a measured pp rate.

As a consequence of points (1) and (2), if for a particular value of $\sin^2 \theta_{12}$ the predicted pp rate as given by the two generation expression is higher than the measured pp rate, then a non-zero θ_{13} can improve the fit. Therefore, lower values of $\sin^2 \theta_{12}$, which are disfavored in the two generation analysis could get allowed in a three generation fit due to non-zero $\sin^2 \theta_{13}$. As a consequence of point (3) we can conclude that if for a particular value of $\sin^2 \theta_{12}$, the two generation predicted pp rate is already higher than the measured pp rate, then a non-zero $\sin^2 \theta_{13}$ which further lowers the pp rate, will not be favored by the fit. We see from the figure 6 that the two generation predicted pp rate exceeds 0.72 below $\sin^2 \theta_{12} \lesssim 0.27$. Therefore for this case a non-zero $\sin^2 \theta_{13}$ improves the fit for all values of $\sin^2 \theta_{12} \lesssim 0.27$. Thus very low values of $\sin^2 \theta_{12}$ which were disfavored by the two generation analysis, could get allowed by $\sin^2 \theta_{13}$, driving the lower allowed limit of $\sin^2 \theta_{12}$ to lower values. For the higher values of $\sin^2 \theta_{12}$, the predicted two generation rate is already lower than 0.72, and therefore non-zero θ_{13} does not change the upper allowed limit of $\sin^2 \theta_{12}$. The predicted two generation pp rate is lower than the measured pp rate of 0.77 only for very low values of $\sin^2 \theta_{12}$, which are already disfavored by the current data. Consequently a non-zero $\sin^2 \theta_{13}$ is not expected to make any impact for this sample case of the measured pp rate from the analysis of the global neutrino data. For the case where the measured pp rate is 0.68, the predicted two generation rate stays higher than 0.68 for $\sin^2 \theta_{12} \lesssim 0.34$ and non-zero $\sin^2 \theta_{13}$ can improve the fit over a large range of $\sin^2 \theta_{12}$. This explains why the lower bound weakens remarkably with

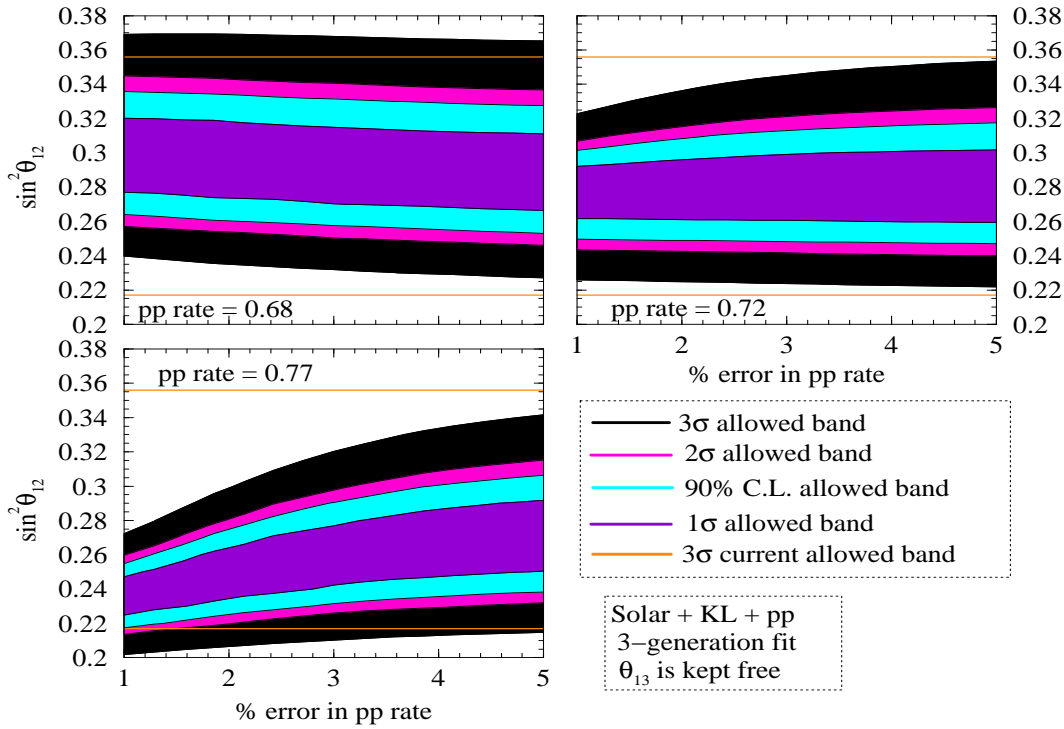


Figure 7: Same as Figure 3 but for a three generation analysis including all neutrino data and keeping $\sin^2 \theta_{13}$ free. We also show the 3σ allowed band of $\sin^2 \theta_{12}$ from the current data.

$\sin^2 \theta_{13}$ in Figure 5. The upper bound is also seen to move towards lower values of $\sin^2 \theta_{12}$. The reason for this can be understood if we remind ourselves that in Figure 5 we do a global analysis of the full solar neutrino data set along with KamLAND and CHOOZ. For the case where we assume that the measured *pp* rate is 0.68, the values of $\sin^2 \theta_{12}$ favored by the *pp* experiment would give a very high predicted rate for CC/NC in SNO and that would be in conflict with the current data. Note also that non-zero $\sin^2 \theta_{13}$ affects the measurement of $\sin^2 \theta_{12}$ by *pp* rate and the CC/NC ratio in SNO in opposite ways – it affects the lower values of $\sin^2 \theta_{12}$ in *pp* experiments and the higher values of $\sin^2 \theta_{12}$ in 8B experiments. Therefore for the case where *pp* rate is 0.68, for which very high values of $\sin^2 \theta_{12} \sim 0.34$ are favored by *pp*, the two generation predicted CC/NC ratio in SNO is ~ 0.34 , much higher than the measured value. However, a non-zero $\sin^2 \theta_{13}$ could reduce this predicted CC/NC ratio in SNO and the *pp* data could be reconciled with the CC/NC data in SNO. This results in the reduction of the global χ^2_{min} . This reduction of the global χ^2_{min} results in the tightening of the upper limit on $\sin^2 \theta_{12}$ for this case.

In figure 7 we depict the $\sin^2 \theta_{12}$ sensitivity as a function of % error in the measured *pp* rate of the world neutrino data including the sample values for the *pp* rate, for the case when θ_{13} is kept free. A comparison of this figure with Figure 3 demonstrates very clearly all the features noted above for the three *pp* rates and for *pp* errors in the range of 1 to 5%. For 0.77 the third mixing angle hardly makes any difference. For 0.72 the lower limit weakens while the upper limit is unaltered. For 0.68 the lower limit weakens but the upper limit improves with the

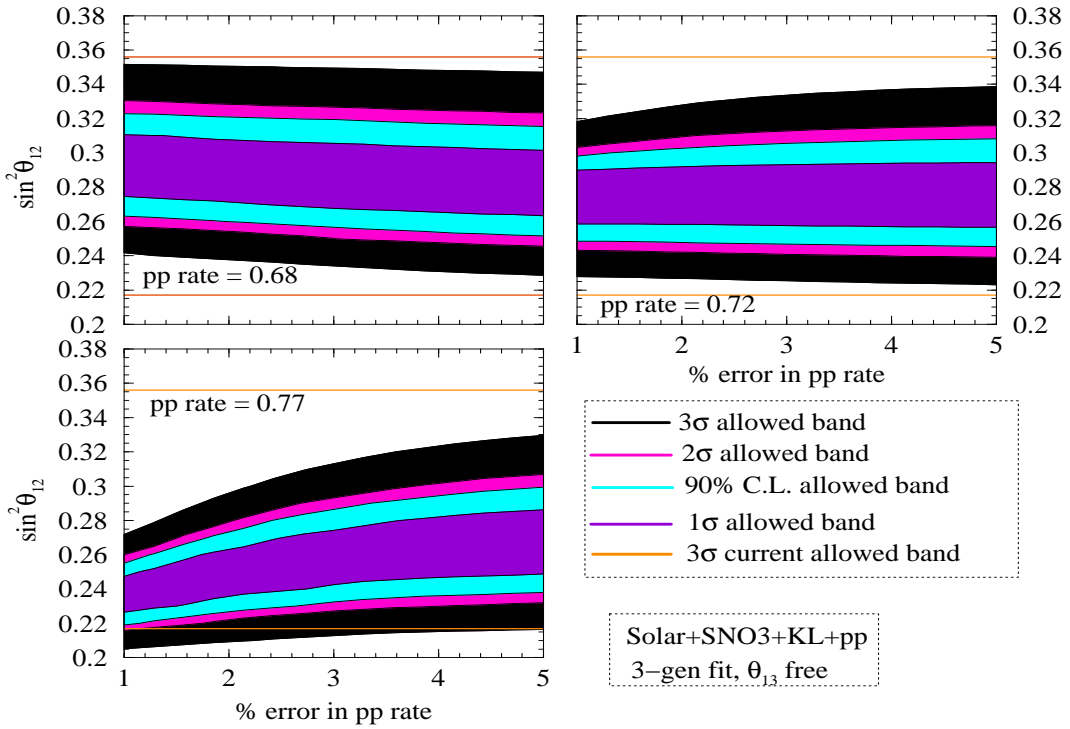


Figure 8: Same as Figure 7 but with the projected error from the third phase of the SNO experiment included. We show the 3σ allowed band from current data.

inclusion of the third generation in the fit. For all the cases the effect of $\sin^2 \theta_{13}$ uncertainty on the $\sin^2 \theta_{12}$ measurement decreases as the error in pp rate increases. Figure 8 shows the corresponding sensitivity plot of $\sin^2 \theta_{12}$ from a three generation analysis of the world neutrino data including both pp rate measurement and projected errors from SNO phase-III.

In Table 3 we give the 3σ ranges and spread obtained from a three generation analysis with and without SNO phase-III. A comparison of the Table 2 and Table 3 bears out the points we have discussed before. However the most important thing to note is that for the most plausible pp rate of 0.72 and 1% error, the uncertainty in the measured value of $\sin^2 \theta_{12}$ increases only from 14% to 17% at 3σ , due to the uncertainty in $\sin^2 \theta_{13}$. From the expression of the three generation oscillation probability Eq. (18), we see that the factor $\cos^4 \theta_{13}$ acts like a ‘‘normalisation constant’’. Since the current 3σ limit on this parameter is $\sin^2 \theta_{13} < 0.05$, one would get a $\sim 10\%$ uncertainty in P_{ee}^{3gen} and would naively expect this uncertainty to show up in the measured value of $\sin^2 \theta_{12}$ using the pp rate. But the actual increase in the $\sin^2 \theta_{12}$ uncertainty due to $\sin^2 \theta_{13}$ is not $\sim 10\%$ but $\sim 3\%$ for the most plausible values of the pp rate. Even for the limiting case of pp rate of 0.68, the increase is only by $\sim 6\%$. The reason is that we determine the value of $\sin^2 \theta_{12}$ not just from the results of the pp experiment alone, but from a combined analysis of the global solar neutrino data. We have stressed before that while the presence of a non-zero value of $\sin^2 \theta_{13}$ would lower the measured value of $\sin^2 \theta_{12}$ from the pp experiment, it would raise the corresponding measured value of $\sin^2 \theta_{12}$ from the 8B experiments. Since these trends are conflicting for the low and high

energy end of the solar neutrino spectrum, the impact of $\sin^2 \theta_{13}$ is much less than what one would naively anticipate. Hence we conclude that the error from $\sin^2 \theta_{13}$ in the $\sin^2 \theta_{12}$ measurement using the pp experiment is only at the few percent level.

However, even though the uncertainty creeping into the $\sin^2 \theta_{12}$ measurement due to $\sin^2 \theta_{13}$ uncertainty is small, the spread expected in $\sin^2 \theta_{12}$ from the pp experiment remain well above the 10% precision level at 3σ . The only type of experiment which could give remarkable precision on $\sin^2 \theta_{12}$ are the reactor experiment tuned to the SPMIN. We discuss this in the next section.

pp rate	% error	solar+reactor +pp		solar(SNO3)+reactor+pp	
		3σ range	spread	3σ range	spread
0.68	1	0.24 - 0.37	21.3%	0.24 - 0.35	18.6%
	2	0.23 - 0.37	23.3%	0.24 - 0.35	18.6%
	3	0.23 - 0.37	23.3%	0.23 - 0.35	20.7%
	4	0.23 - 0.37	23.3%	0.23 - 0.35	20.7%
0.72	1	0.225 - 0.32	17.4%	0.23 - 0.32	16.3%
	2	0.22 - 0.34	21.4%	0.23 - 0.33	17.9 %
	3	0.22 - 0.34	21.4%	0.22 - 0.33	20.0 %
	4	0.22 - 0.35	22.8%	0.22 - 0.34	21.4%
0.77	1	0.2 - 0.27	14.9%	0.21 - 0.27	12.5%
	2	0.21 - 0.30	17.6%	0.21 - 0.29	16.0%
	3	0.21 - 0.32	20.7%	0.21 - 0.31	19.2%
	4	0.21 - 0.33	22.2%	0.21 - 0.32	20.7%

Table 3: The 3σ allowed ranges and % spread of $\sin^2 \theta_{12}$ obtained from a three generation analysis of the all neutrino data including the pp rate.

4 Measuring θ_{12} in a reactor experiment at SPMIN

In this section we expound the possibility of measuring the mixing angle $\sin^2 \theta_{12}$ by detecting reactor anti-neutrinos in a detector placed at a distance which corresponds to a maximum of flavor oscillations or a Survival Probability MINimum (SPMIN). We will consider an experiment similar to the KamLAND experiment, but at a more appropriate baseline – a baseline tuned to the SPMIN. The condition of SPMIN is given by

$$L_{min} \approx 1.24 \frac{E/MeV}{\Delta m_{21}^2 / eV^2} \quad (16)$$

That this kind of experiment is best for the measurement of the mixing angle was proposed in [14]. For the old low-LMA best-fit of $\Delta m_{21}^2 = 7.2 \times 10^{-5} \text{ eV}^2$, the baseline which gives the most accurate measurement of $\sin^2 \theta_{12}$ was found to be 70 km, which corresponds to the appearance of SPMIN

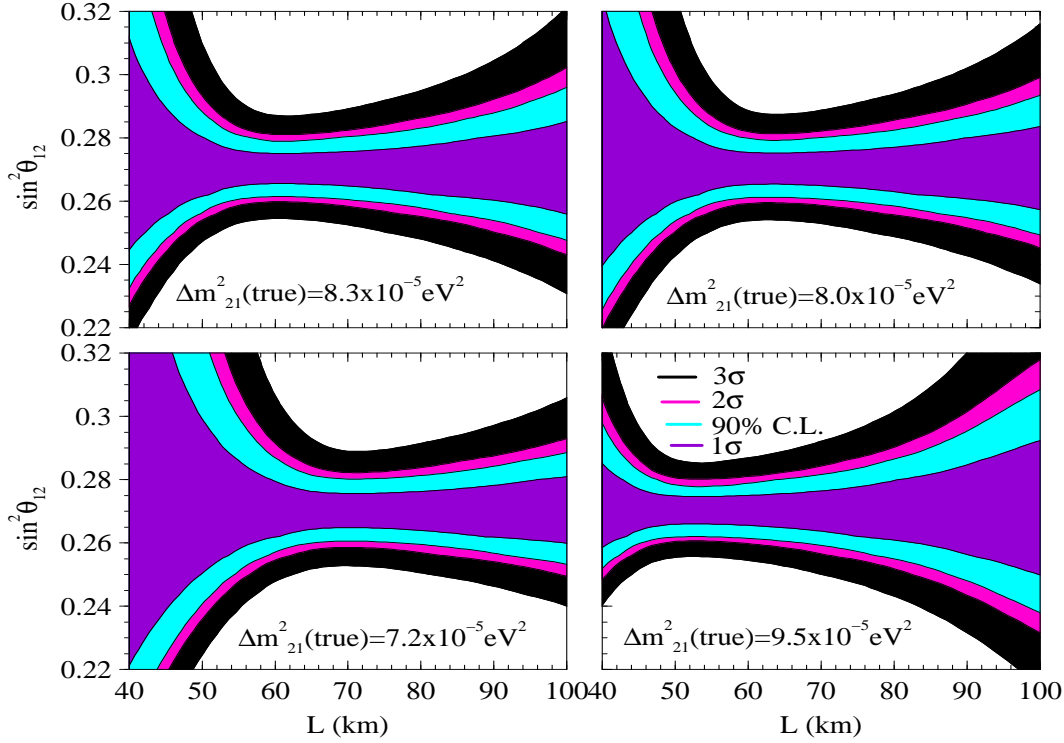


Figure 9: Sensitivity plots showing the 1σ , 1.64σ , 2σ , and 3σ range of allowed values for $\sin^2 \theta_{12}$ as a function of the baseline L . The 4 panels are for 4 different true value of Δm_{21}^2 . The true value of $\sin^2 \theta_{12}$ is assumed to be 0.27 in all the cases. The Δm_{21}^2 is allowed to vary freely in the fit.

at the positron prompt energy $E_{vis} = 3.2$ MeV,⁴ close to where the reactor anti-neutrino flux is highest and therefore statistically most relevant in the observed positron spectrum. Now that the best-fit value of Δm_{21}^2 is somewhat different, we expect that the SPMIN would appear in the statistically most relevant part of the spectrum for a slightly different baseline. We find that for $\Delta m_{21}^2 = 8.3 \times 10^{-5}$ eV 2 , $\sin^2 \theta_{12}$ could be measured with an accuracy of $\sim 2(6)\%$ at $1\sigma(3\sigma)$ if the baseline was taken as ~ 60 km, for which the SPMIN appears at $E_{vis} = 3.2$ MeV in the positron spectrum. In this section we extend our earlier work by probing in detail the dependence of the precision of $\sin^2 \theta_{12}$ measurement on the true value of Δm_{21}^2 , the baseline, the statistics and the systematics of the experiment. We also compare the results of the two-generation analyses with a full three-generation calculation, where the unknown parameter $\sin^2 \theta_{13}$ is allowed to vary freely within its current allowed range. We quantitatively study the error introduced in the measured value of $\sin^2 \theta_{12}$ due to all these above factors. We discuss the relevance of the geo-neutrino flux on the precision of $\sin^2 \theta_{12}$ measurement.

⁴For the details of our reactor code and statistical analysis, we refer the reader to our earlier papers [14, 31, 32].

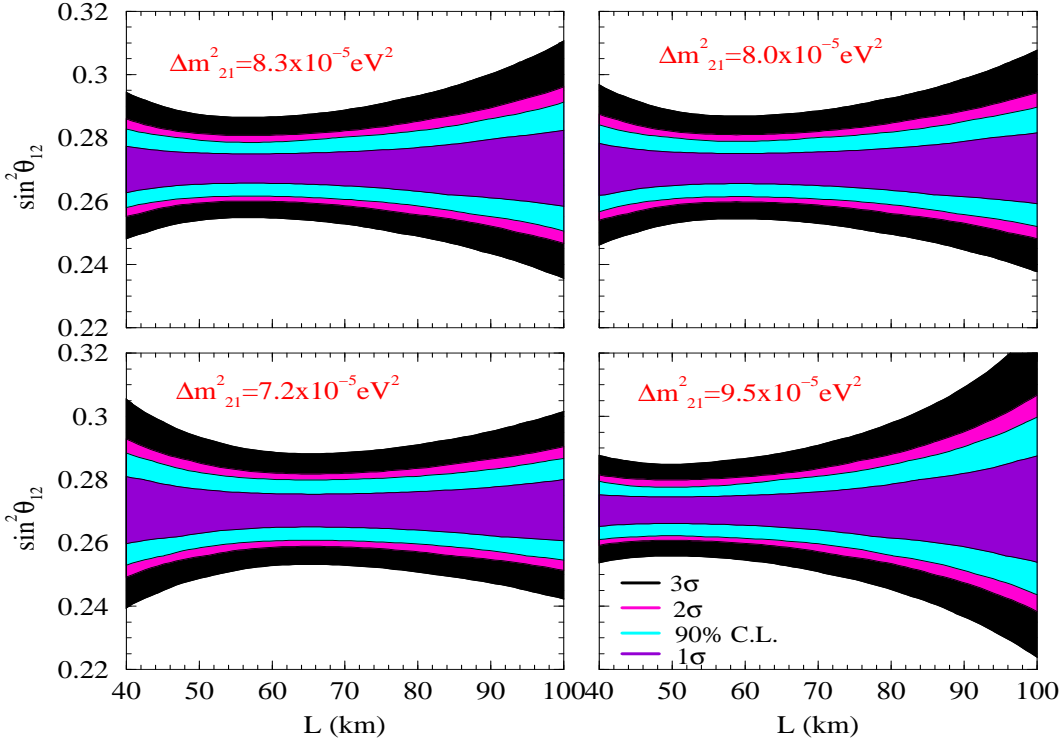


Figure 10: Same as Figure 9 but in this figure the Δm_{21}^2 was kept fixed at its assumed true value in each of the panels.

4.1 Sensitivity to $\sin^2 \theta_{12}$ and the baseline

In Figure 9 we show the $\sin^2 \theta_{12}$ sensitivity expected in a reactor experiment as a function of the baseline L . We assume a total systematic uncertainty of 2% and consider a statistics of 73 GWkTy (given as a product of reactor power in GW and the exposure of the detector in kTy). We have assumed that the detector composition is same as that of KamLAND and so it has the same number of target protons per kton as KamLAND. Note that the total reactor power and the detector size and exposure is kept same for all baselines. Therefore for longer baseline the number of events would fall as the inverse square law. We assume that the true value of $\sin^2 \theta_{12} = 0.27$ and simulate the prospective observed positron spectrum in the detector for four different assumed true values of Δm_{21}^2 . We take $\sin^2 \theta_{13} = 0$ for this figure. We define a χ^2 function given by

$$\chi^2 = \sum_{i,j} (N_i^{data} - N_i^{theory})(\sigma_{ij}^2)^{-1}(N_j^{data} - N_j^{theory}) , \quad (17)$$

where N_i^α ($\alpha = data, theory$) is the number of events in the i^{th} bin, σ_{ij}^2 is the covariant error matrix containing the statistical and systematic errors and the sum is over all bin. We use this χ^2 to fit back the simulated spectrum data to get the measured value of $\sin^2 \theta_{12}$, keeping Δm_{21}^2 free. We simulate the spectrum at each baseline and plot the range of values of $\sin^2 \theta_{12}$ allowed by the experiment as a function of the baseline. The baseline at which the band of allowed values of

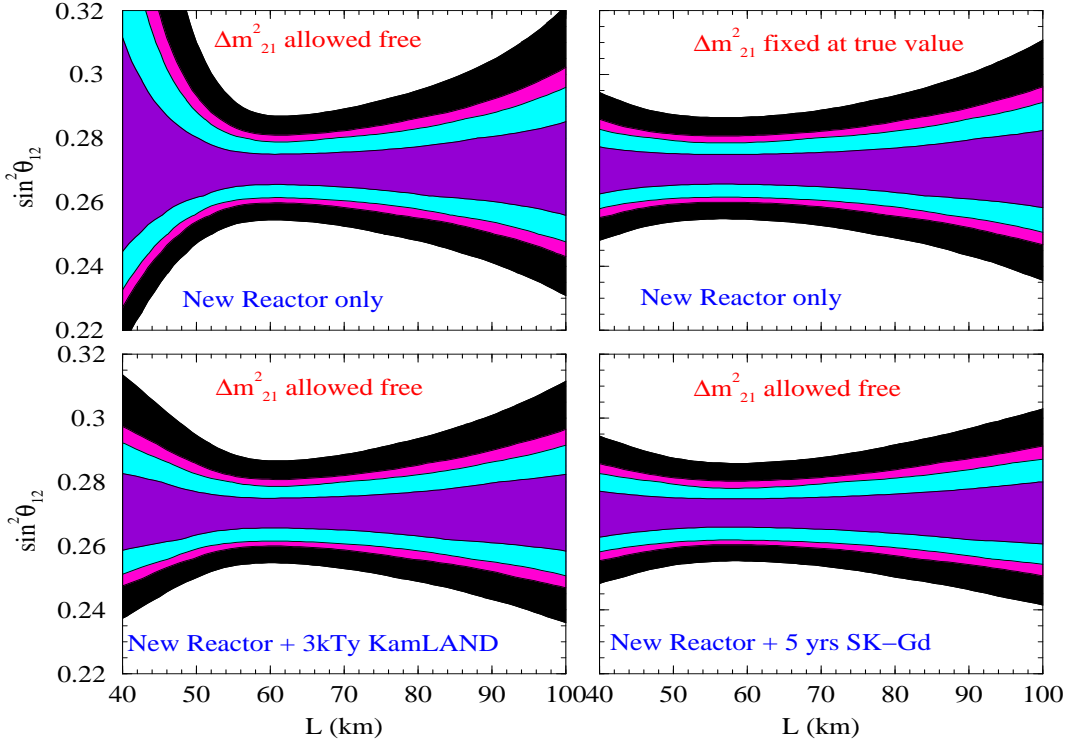


Figure 11: Sensitivity plots showing the 1σ , 1.64σ , 2σ , and 3σ range of allowed values for $\sin^2 \theta_{12}$ as a function of the baseline L . The true value of $\Delta m_{21}^2(\text{true}) = 8.3 \times 10^{-5} \text{ eV}^2$ and $\sin^2 \theta_{12}(\text{true}) = 0.27$ for all panels. The upper left (right) hand panel is same as the upper left hand panel in Figure 9 (10). The lower left hand panel is for combined analysis of the 73 GWkTy data from the new SPMIN reactor experiment and 3 kTy data from KamLAND. The lower right hand panel shows the projected sensitivity for 73 GWkTy data from the new SPMIN reactor experiment and 5 years data from the proposed SK-Gd experiment.

$\sin^2 \theta_{12}$ is most narrow is the ideal baseline for the SPMIN reactor experiment. The figure confirms that this ideal baseline depends crucially on the true value of Δm_{21}^2 , since the condition of SPMIN depends on the true value of Δm_{21}^2 (cf. Eq. (16)). The most optimal baseline for the true value of $\Delta m_{21}^2 = 8.3(8.0) \times 10^{-5} \text{ eV}^2$ is seen to be 60(63) km from the Figure 9, while for the old low-LMA best-fit of $\Delta m_{21}^2 = 7.2 \times 10^{-5} \text{ eV}^2$ the best baseline would be 70 km. At the most optimal baseline the SPMIN reactor experiment can achieve an unprecedented accuracy of $\sim 2(6)\%$ at $1\sigma(3\sigma)$ in the measurement of $\sin^2 \theta_{12}$.

From the Figure 9 we get an impression that the optimal baseline for a given true value of Δm_{21}^2 is very finely tuned. For instance, for $\Delta m_{21}^2(\text{true}) = 8.3 \times 10^{-5} \text{ eV}^2$, if we change the baseline from $L = 60$ to $L = 50$ km, the sensitivity in $\sin^2 \theta_{12}$ decreases from $\sim 2(6)\%$ to $\sim 3(11)\%$ at $1\sigma(3\sigma)$. However, note that in Figure 9 we had allowed Δm_{21}^2 to vary freely. Therefore both $\sin^2 \theta_{12}$ and Δm_{21}^2 were being effectively determined by this new reactor SPMIN experiment alone. For some baselines, especially at smaller L , the oscillation induced spectral distortion is not enough to measure Δm_{21}^2 accurately, while for the longer baselines the statistics are lower. These factors

lead to uncertainty in the measurement of Δm_{21}^2 within this experimental set-up. The uncertainty in the Δm_{21}^2 measurement translates to extra uncertainty in the $\sin^2 \theta_{12}$ measurement. If Δm_{21}^2 could be fixed, assumed to be measured to a very high precision in some other experiment, then the uncertainty in $\sin^2 \theta_{12}$ due to Δm_{21}^2 can be gotten rid of. In Figure 10 we show the sensitivity plot as in Figure 9, but in this case we fix Δm_{21}^2 at its assumed true value for each of the panels. We can note that if Δm_{21}^2 was kept fixed, then the choice of the baseline for setting up the SPMIN experiment becomes much broader. For instance, for the fixed Δm_{21}^2 case, we can see from Figure 10 that for $\Delta m_{21}^2(\text{true}) = 8.3 \times 10^{-5} \text{ eV}^2$, if we change the baseline from $L = 60$ to $L = 70$ km, the sensitivity in $\sin^2 \theta_{12}$ decreases only from 6.1% to only 6.3% at 3σ .

Indeed we expect Δm_{21}^2 to be measured with reasonable accuracy in the future experiments. The KamLAND experiment is expected to measure Δm_{21}^2 with about 7% accuracy with 3 kTy data [24, 14, 12]. The proposed SK-Gd experiment (Gadzooks! [33]) has the potential to determine the true value of Δm_{21}^2 within $\sim 2 - 3\%$ [32]. In Figure 11 we show the sensitivity on $\sin^2 \theta_{12}$ expected if we combine the SPMIN reactor data with 3 kTy prospective data from KamLAND (lower left panel) and 5 years simulated data from the proposed SK-Gd (lower right panel). The upper panels are for the data from the SPMIN reactor experiment alone. For all the panels we have assumed $\Delta m_{21}^2(\text{true}) = 8.3 \times 10^{-5} \text{ eV}^2$. In the upper left panel we allow Δm_{21}^2 to vary freely while in the upper right panel Δm_{21}^2 is fixed at the assumed true value. We note that if the SPMIN reactor data is combined with 5 years of data from the SK-Gd experiment, we have a much wider choice for the baseline as in the Δm_{21}^2 fixed case, since Δm_{21}^2 is determined extremely accurately by SK-Gd. With the addition of the SK-Gd results to the total data set, the spread in $\sin^2 \theta_{12}$ improves marginally to $\sim 5.7\%$ at 3σ . The SPMIN reactor and 3 kTy KamLAND data combined would yield a sensitivity in $\sin^2 \theta_{12}$ of $\sim 5.9\%$ at 3σ . Since for SK-Gd and SPMIN reactor combined analysis we have confirmed that the effect of Δm_{21}^2 on the $\sin^2 \theta_{12}$ sensitivity can be neglected, we will take Δm_{21}^2 to be fixed for the remainder of this section.

4.2 Impact of statistics and systematics on $\sin^2 \theta_{12}$ sensitivity

One of the driving features for this kind of a precision experiment is the statistics. Since the statistics falls as the inverse square law and since we need relatively longer baselines for measuring the solar neutrino oscillation parameters, this implies that for given reactor power we would need bigger detectors and larger exposure times for longer baselines. Therefore its plausible to ask at this point the question: *How much do we loose on the $\sin^2 \theta_{12}$ sensitivity due to statistics as we increase the baseline to tune to the SPMIN?* In Figure 12 we show this effect of changing the statistics on the $\sin^2 \theta_{12}$ sensitivity for the case where true value of $\Delta m_{21}^2(\text{true}) = 8.3 \times 10^{-5} \text{ eV}^2$. For the four panels we take four different sample baselines of 50, 60, 70 and 80 km and plot the band of allowed values of $\sin^2 \theta_{12}$ as a function of the product of reactor power and the detector mass and exposure time. In the panel for $L = 60$ km we note that the sensitivity of $\sin^2 \theta_{12}$ improves from 3(10)% to 2(6)% at $1\sigma(3\sigma)$ as the statistics is increased from 20 GWkTy to 60 GWkTy. Note that the difference in the $\sin^2 \theta_{12}$ precision for 60 GWkTy and 73 GWkTy (used in Figures 9 and 10) is marginal, and shows up only in the first place in decimal in the value of the spread.

Another important aspect which determines the potential of the experiment to precision mea-

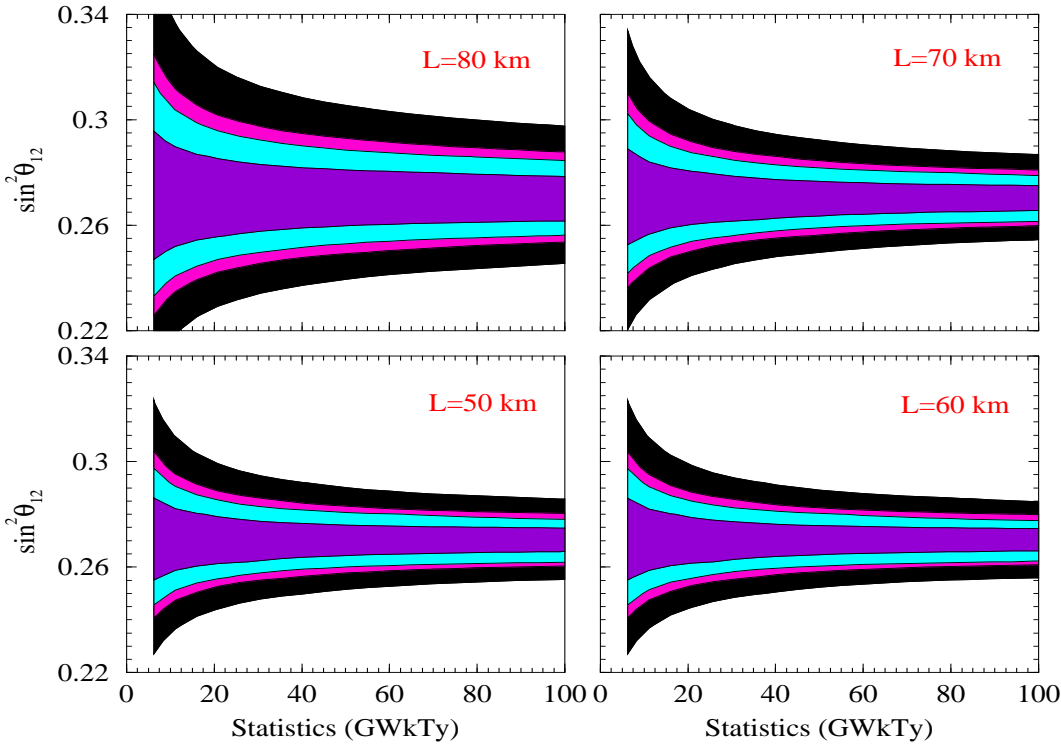


Figure 12: Sensitivity plots showing the 1σ , 1.64σ , 2σ , and 3σ range of allowed values for $\sin^2 \theta_{12}$ as a function of the statistics in units of GWkTy . All the four panels correspond to a fixed value of $\Delta m_{21}^2 = 8.3 \times 10^{-5} \text{ eV}^2$.

surement is the systematic uncertainty. Obviously lower systematics should be preferable. All the plots presented in this section so far have been generated with an assumed 2% systematic uncertainty. The systematic uncertainty in the KamLAND experiment is about 6.5%, bulk of which comes from the uncertainty on the detector fiducial mass and the reactor power. Our assumption of 2% systematics is an optimistic choice where we have assumed that the error on the flux normalisation could be reduced remarkably by using the near-far detector set-up. One could envisage the θ_{12} reactor SPMIN experiment as a second leg of a dedicated reactor experiment to measure θ_{13} . The detector for measuring θ_{13} could then effectively work as the near detector for the long baseline SPMIN experiment for θ_{12} . However, in addition to that, the error coming from uncertainty on energy threshold and neutrino spectra have to be reduced to achieve this very optimistic systematics of 2%. Experimentally this could be a very challenging task.

Since systematic uncertainties are always difficult to reduce in these kind of experiments, we give here an estimate of how much the precision on $\sin^2 \theta_{12}$ deteriorates as the systematic uncertainties increase. Figure 13 shows the effect of increasing the systematic uncertainty from our optimistic assumption of 2% to a very conservative estimate of 5%. For $\Delta m_{21}^2(\text{true}) = 8.3 \times 10^{-5} \text{ eV}^2$, the spread in $\sin^2 \theta_{12}$ at $L = 60 \text{ km}$ increases from 6.1% to 8.6% at 3σ , as the systematic error is increased from 2% to 5%. We conclude that the effect of systematic uncertainty on the precision of $\sin^2 \theta_{12}$ measurement is important, but the impact is not catastrophic.

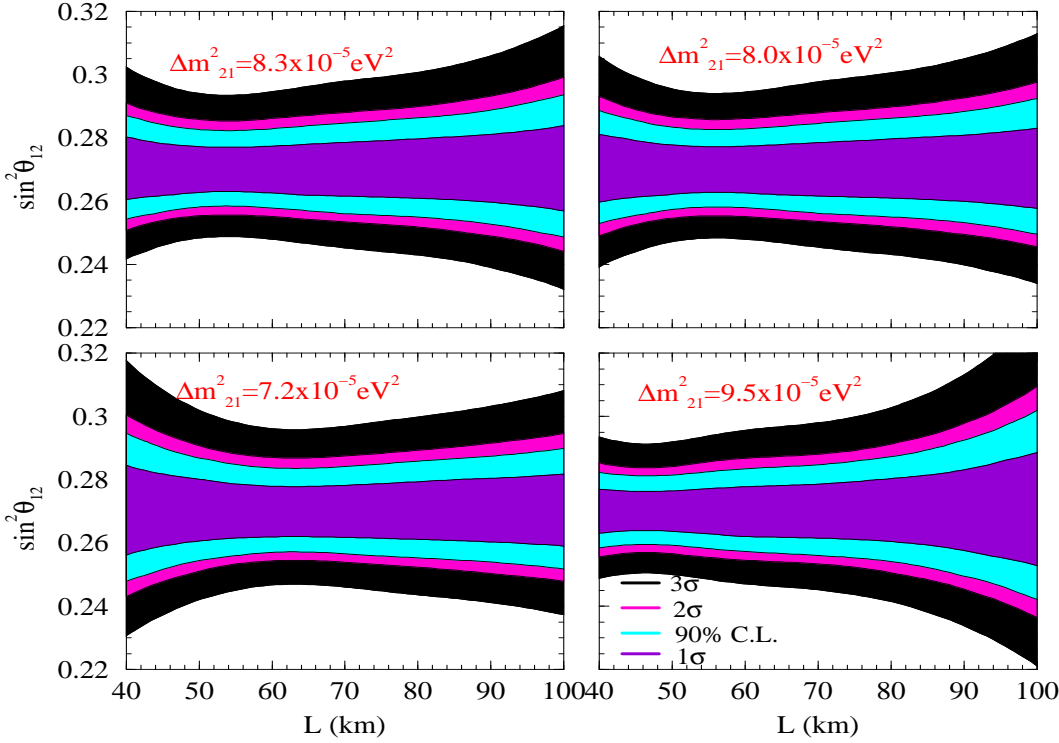


Figure 13: Same as Figure 10 but for a systematic uncertainty of 5%.

4.3 Uncertainty in $\sin^2 \theta_{12}$ due to uncertainty in $\sin^2 \theta_{13}$

So far we had assumed that the true value of $\theta_{13} = 0$. However we do not have any experimental information yet on the true value of this parameter. From the combined analysis of all existing data from reactor (CHOOZ, Palo Verde, KamLAND), solar and atmospheric neutrinos we can put an upper limit on this parameter of $\sin^2 \theta_{13} < 0.05$ at 3σ [12, 13]. As discussed before in connection with KamLAND, the full three-generation survival probability for the reactor anti-neutrinos is given by

$$P_{ee} \approx \cos^4 \theta \left(1 - \sin^2 2\theta_{12} \sin^2 \frac{\Delta m_{21}^2 L}{4 E_\nu} \right), \quad (18)$$

where we have neglected the term $\sim \sin^4 \theta$. Therefore the uncertainty in $\sin^2 \theta_{13}$ essentially brings up to a $\sim 10\%$ uncertainty in the $\bar{\nu}_e$ survival probability. Since the factor $\cos^4 \theta$ can only reduce the survival probability, it does not affect the upper limit on the allowed range of $\sin^2 \theta_{12}$. However, it can have an effect on the lower limit on $\sin^2 \theta_{12}$ reducing it further, and thus can worsen, in principle, the precision of the experiment.

How much do we lose on the $\sin^2 \theta_{12}$ sensitivity due to the uncertainty in the value of $\sin^2 \theta_{13}$?
 The additional error on $\sin^2 2\theta_{12}$ coming from the uncertainty on $\sin^2 \theta_{13}$ can be roughly estimated

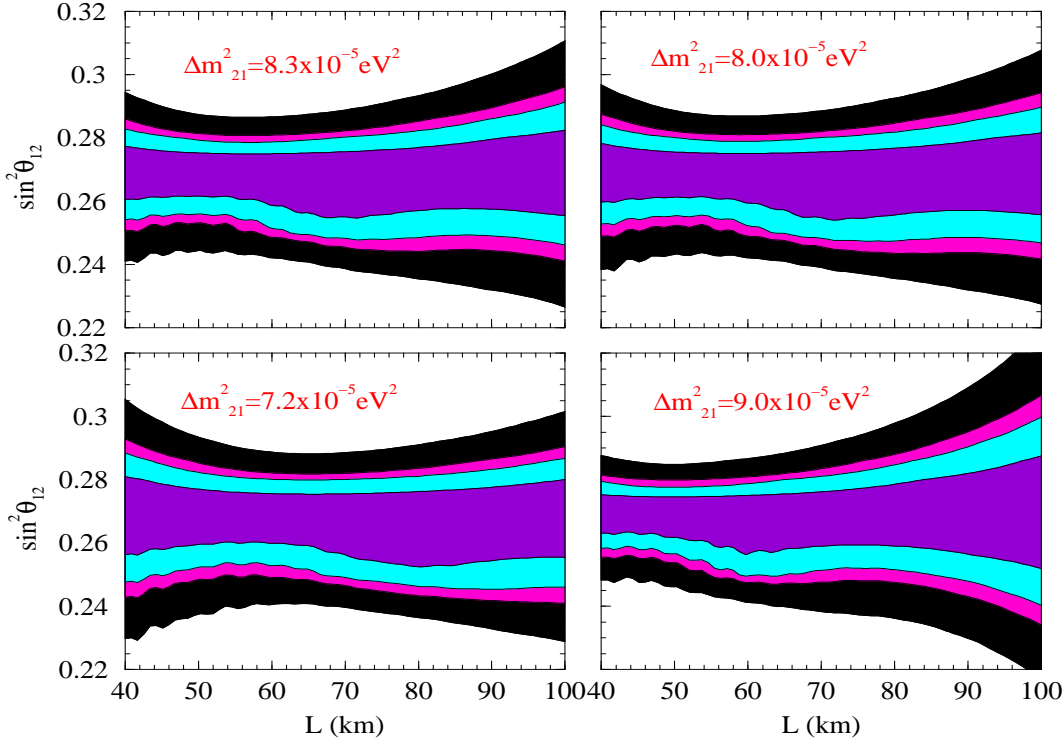


Figure 14: Same as Figure 10 but for a three generation analysis where $\sin^2 \theta_{13}$ is allowed to vary freely within its current 3σ allowed range.

using Eq. (18) as,

$$\delta(\sin^2 2\theta_{12}) \approx \frac{2\Delta P_{ee} \sin^2 \theta_{13}}{\sin^2 \frac{\Delta m_{21}^2 L}{4E_\nu}} + 2 \frac{(1 - \sin^2 2\theta_{12} \sin^2 \frac{\Delta m_{21}^2 L}{4E_\nu}) \Delta(\sin^2 \theta_{13})}{\sin^2 \frac{\Delta m_{21}^2 L}{4E_\nu}}, \quad (19)$$

where ΔP_{ee} and $\Delta(\sin^2 \theta_{13})$ are the uncertainties in the determination of the survival probability and $\sin^2 \theta_{13}$, respectively. We work in a scenario in which one would use the SPMIN in order to determine $\sin^2 2\theta_{12}$. In the SPMIN region one has $\sin^2(\Delta m_{21}^2 L / 4E_\nu) \sim 1$ and therefore

$$\delta(\sin^2 2\theta_{12}) \approx 2\Delta P_{ee} \sin^2 \theta + 2 \cos^2 2\theta_{12} \Delta(\sin^2 \theta_{13}). \quad (20)$$

Thus, in this SPMIN scenario, the first term gives an extra contribution of about $2\Delta P_{ee} \sin^2 \theta$ to the allowed range of $\sin^2 2\theta_{12}$. Even under the most conservative conditions $\Delta P_{ee} \lesssim 0.1$, and this term gives an extra contribution of $\lesssim 0.01$ to the allowed range of $\sin^2 2\theta_{12}$. The second term is independent of the precision of a given experiment and depends only on the best-fit value of $\cos^2 2\theta_{12}$ and on the error in $\sin^2 \theta_{13}$. For the current 3σ error in $\sin^2 \theta_{13}$ of 0.05 and best-fit $\cos^2 2\theta_{12}$ of 0.19, this would give an increase of only about 0.02. The suppression of this term is mainly due to the presence of the $\cos^2 2\theta_{12}$ factor, which is a relatively small number for the current best-fit solution. Thus, even though the uncertainty in $\sin^2 \theta_{13}$ brings a 10% uncertainty

in the value of P_{ee} , it increases the allowed range of $\sin^2 2\theta_{12}$ only by a few %, if one uses the SPMIN region for the $\sin^2 2\theta_{12}$ determination.

In Figure 14 we show the sensitivity in $\sin^2 \theta_{12}$ that we expect for the case when θ_{13} is allowed to vary freely in its currently allowed range of $\sin^2 \theta_{13} < 0.05$. The figure confirms that the upper bound on $\sin^2 \theta_{12}$ remains unaffected by the $\sin^2 \theta_{13}$ uncertainty, while the lower limit weakens somewhat, increasing the $\sin^2 \theta_{12}$ uncertainty. However for the baseline which corresponds to the SPMIN, the sensitivity reduces only by 2–3% due to the 10% uncertainty in $\sin^2 \theta_{13}$. As a concrete example, for $\Delta m_{21}^2(\text{true}) = 8.3 \times 10^{-5} \text{ eV}^2$ the uncertainty in $\sin^2 \theta_{12}$ worsens from 6.1% to 8.7% at 3σ .

4.4 Impact of the geo-neutrino flux

Our earth is known to be a huge heat reservoir and is estimated to radiate about 40 TW of heat. A large fraction ($\sim 16\%$) of this is believed to be radiogenic in origin, coming from the decay chain of ^{238}U , ^{232}Th and ^{40}K . Radioactive decay of these isotopes produce antineutrinos in the beta decay processes of their decay chain. These $\bar{\nu}_e$ coming from inside the earth are usually called the Geo-neutrinos ($\bar{\nu}_{geo}$) [34]. Since the maximum energy of the $\bar{\nu}_{geo}$ produced in the ^{40}K decay chain is only $E_{\bar{\nu}_e} = 1.31 \text{ MeV}$, these are below the detection threshold of $\bar{\nu}_e$ in scintillation detectors and therefore undetectable. However the $\bar{\nu}_{geo}$ from ^{238}U and ^{232}Th have maximum energy of $E_{\bar{\nu}_e} = 3.26 \text{ MeV}$ and $E_{\bar{\nu}_e} = 2.25 \text{ MeV}$ respectively and can be observed in scintillation detectors.

The flux of $\bar{\nu}_{geo}$ are largely unknown. Even the total heat radiated by earth has a huge uncertainty and could be between 31–40 TW. There is no direct measure of the abundance of the ^{238}U and ^{232}Th inside the earth and one can only estimate their abundance using the meteoritic and seismic data. This results in the $\bar{\nu}_{geo}$ being largely model dependent and extremely uncertain. However, most models give the bulk $^{232}Th/^{238}U$ ratio as $^{232}Th/^{238}U \sim 3.8$. But even this ratio could have a large enough error (eg. the authors of [35] estimate this error as 14%). Observation of these $\bar{\nu}_{geo}$ events would lead to a better understanding of the interior of our earth, and is therefore a very important branch of neutrino physics in its own right [36]. However, as far as the precision measurement of the neutrino oscillation parameters is concerned, the $\bar{\nu}_{geo}$ events form a formidable background and can lead to error in the values of $\sin^2 \theta_{12}$ determined.

Since the $\bar{\nu}_{geo}$ have a maximum energy of only 2.48 MeV, one way to avoid the uncertainty coming from them is to put a prompt energy threshold of 2.6 MeV, as done by the KamLAND collaboration. In this paper we have followed that approach. In this approach the observed positron spectrum is *clean*, without any contamination from $\bar{\nu}_{geo}$. Another approach is to use the entire prompt energy spectrum in the analysis, taking the $\bar{\nu}_{geo}$ flux into account. Since the theoretical estimates on the $\bar{\nu}_{geo}$ flux are rather poor at the moment, the best way would be to let the ^{238}U and ^{232}Th flux normalisation vary as a free parameter. Both approaches could have their merits and demerits. For the first approach (which we use in this paper), while there are no extra uncertainties coming from the unknown $\bar{\nu}_{geo}$ background, one has to contend with the experimental challenge of understanding and reducing the error coming from the prompt energy threshold. For the second approach, while there is no prompt energy cut, one has to handle the uncertainty coming from the lack of knowledge of the $\bar{\nu}_{geo}$ background. (Keeping the ^{238}U and ^{232}Th flux normalisation as free parameters brings in extra error in the measurement on $\sin^2 \theta_{12}$.)

The key feature in the θ_{12} SPMIN reactor experiment that we are proposing is the appearance of the SPMIN in the observed positron spectrum. If this SPMIN appears at a prompt energy of $E_{vis} > 2.6$ MeV, then it could be a better idea to put a detector threshold of $E_{vis} = 2.6$ MeV and avoid the $\bar{\nu}_{geo}$ background.⁵ If on the other hand, SPMIN appears at $E_{vis} < 2.6$ MeV, then one has to take the entire positron energy spectrum into account and in this case the $\bar{\nu}_{geo}$ background cannot be avoided. For a given value of Δm_{21}^2 , the position of SPMIN in the $\bar{\nu}_e$ spectrum depends on the baseline of the experiment. For shorter baselines, SPMIN occurs at smaller energies. Therefore the baseline of the experiment would determine whether one is forced to take the $\bar{\nu}_{geo}$ background into account or not.

Before we conclude, we would like to point out that the authors of [37] have included the $\bar{\nu}_{geo}$ background in their analysis of the $\sin^2 \theta_{12}$ precision expected in a specific 54 km baseline θ_{12} SPMIN experiment in Japan (which they call SADO). They conclude, that for this experimental set-up the $\bar{\nu}_{geo}$ background does not have much impact on the $\sin^2 \theta_{12}$ precision. However, one should note that for the baseline of 54 km, the SPMIN comes at $E_{vis} \cong 2.8$ MeV. Since this is above the $\bar{\nu}_{geo}$ background anyway, the $\bar{\nu}_{geo}$ uncertainty does not make much impact for this case. However, for shorter baselines where the SPMIN comes at $E_{vis} < 2.6$ MeV, the uncertainty due to the $\bar{\nu}_{geo}$ flux will seriously start affecting the $\sin^2 \theta_{12}$ precision.

5 Conclusions

We have investigated the possibilities of high precision measurement of the solar neutrino mixing angle θ_{12} in solar and reactor neutrino experiments. As a first step, we have analyzed the improvements in the determination of $\sin^2 \theta_{12}$, which can be achieved with the expected increase of statistics and reduction of systematic errors in the currently operating solar and KamLAND experiments. With the phase-III prospective data from SNO experiment included in the current global solar neutrino and KamLAND data, the uncertainty in the value of $\sin^2 \theta_{12}$ is expected to diminish from 24% to 21% at 3σ . If instead of 766.3 Ty, one uses simulated 3 kTy KamLAND data in the same analysis, the 3σ error in $\sin^2 \theta_{12}$ reduces to 18%.

We next considered the potential of a generic LowNu $\nu - e$ elastic scattering experiment, designed to measure the pp solar neutrino flux, for high precision determination of $\sin^2 \theta_{12}$. We examined the effect of including values of the pp neutrino induced electron scattering rates in the χ^2 analysis of the global solar neutrino data. Three representative values of the rates from the currently allowed 3σ range were considered: 0.68, 0.72, 0.77. The error in the measured rate was varied from 1% to 5%. By adding the pp flux data in the analysis, the error in $\sin^2 \theta_{12}$ determination reduces to 14% (19%) at 3σ for 1% (3%) uncertainty in the measured pp rate. Performing a similar three-neutrino oscillation analysis we found that, as a consequence of the uncertainty on $\sin^2 \theta_{13}$, the error on the value of $\sin^2 \theta_{12}$ increases correspondingly to 17% (21%).

We also studied the possibility of a high precision determination of $\sin^2 \theta_{12}$ in a reactor experiment with a baseline corresponding to a Survival Probability MINimum (SPMIN). We showed that in a $L \sim 60$ km experiment with statistics of ~ 60 GWkTy and systematic error of 2%, $\sin^2 \theta_{12}$

⁵This will increase the systematic uncertainty due to the error from the prompt energy cut. However, we have shown that the impact of the increase of the systematic uncertainty on $\sin^2 \theta_{12}$ is not very large.

could be measured with an uncertainty of 2% (6%) at 1σ (3σ). The inclusion of the $\sin^2 \theta_{13}$ uncertainty in the analysis changes this error to 3% (9%). We investigated in detail the dependence of the precision on $\sin^2 \theta_{12}$ which can be achieved in such an experiment on the baseline, statistics and systematic error. More specifically, with the increase of the statistics from 20 GWkTy to 60 GWkTy, the error diminishes from 3% (10%) to 2% (6%) at 1σ (3σ). For statistics of (60 - 70) GWkTy, the increase of the systematic error from 2% to 5% leads to an increase in the uncertainty in $\sin^2 \theta_{12}$ from 6% to 9% at 3σ .

We have found that the effect of $\sin^2 \theta_{13}$ uncertainty on the $\sin^2 \theta_{12}$ determination in LowNu *pp* and SPMIN reactor experiments considered is considerably smaller than naively expected.

The results of our analyses for the currently running, the proposed LowNu and future reactor experiments show that the most precise determination of $\sin^2 \theta_{12}$ can be achieved in a dedicated reactor experiment with a baseline tuned to SPMIN.

Acknowledgments: We would like to thank Y. Suzuki, A. Suzuki, M. Nakahata, F. Suekane, and C. Peña-Garay for useful discussions. This work was supported by the Italian INFN under the program “Fisica Astroparticellare” (S.C. and S.T.P.).

References

- [1] B. T. Cleveland *et al.*, *Astrophys. J.* **496**, 505 (1998).
- [2] J. N. Abdurashitov *et al.* [SAGE Collaboration], *J. Exp. Theor. Phys.* **95**, 181 (2002) [Zh. Eksp. Teor. Fiz. **122**, 211 (2002)] [arXiv:astro-ph/0204245]. ; W. Hampel *et al.* [GALLEX Collaboration], *Phys. Lett. B* **447**, 127 (1999) ; C. Cattadori, Talk at Neutrino 2004, Paris, France, June 14-19, 2004.
- [3] S. Fukuda *et al.* [Super-Kamiokande Collaboration], *Phys. Lett. B* **539**, 179 (2002) [arXiv:hep-ex/0205075].
- [4] Q. R. Ahmad *et al.* [SNO Collaboration], *Phys. Rev. Lett.* **89**, 011301 (2002) [arXiv:nucl-ex/0204008]; Q. R. Ahmad *et al.* [SNO Collaboration], *Phys. Rev. Lett.* **89**, 011302 (2002) [arXiv:nucl-ex/0204009].
- [5] S. N. Ahmed *et al.* [SNO Collaboration], *Phys. Rev. Lett.* **92**, 181301 (2004) [arXiv:nucl-ex/0309004].
- [6] E. Kearns, talk at Neutrino 2004, Paris, <http://neutrino2004.in2p3.fr>.
- [7] K. Eguchi *et al.*, [KamLAND Collaboration], *Phys. Rev. Lett.* **90** (2003) 021802 [arXiv:hep-ex/0212021].
- [8] M.H. Ahn *et al.*, *Phys. Rev. Lett.* **90** (2003) 041801.
- [9] T. Araki *et al.*, [KamLAND Collaboration], hep-ex/0406035.

- [10] T. Nakaya *et al.*, talk given at ν '04 International Conference, June 14-19, 2004, Paris, France
- [11] V. Gribov and B. Pontecorvo, Phys. Lett. **B28**, 493 (1969).
- [12] A. Bandyopadhyay, S. Choubey, S. Goswami, S. T. Petcov and D. P. Roy, hep-ph/0406328.
- [13] M. Maltoni, T. Schwetz, M. A. Tortola and J. W. F. Valle, arXiv:hep-ph/0405172; J. N. Bahcall, M. C. Gonzalez-Garcia and C. Pena-Garay, JHEP **0408**, 016 (2004) [arXiv:hep-ph/0406294]. P. Aliani, V. Antonelli, R. Ferrari, M. Picariello and E. Torrente-Lujan, arXiv:hep-ph/0406182.
- [14] A. Bandyopadhyay, S. Choubey and S. Goswami, Phys. Rev. D **67**, 113011 (2003) [arXiv:hep-ph/0302243].
- [15] A. Bandyopadhyay, S. Choubey, S. Goswami and S. T. Petcov, Phys. Lett. B **581**, 62 (2004) [arXiv:hep-ph/0309236].
- [16] J. N. Bahcall and C. Pena-Garay, JHEP **0311**, 004 (2003) [arXiv:hep-ph/0305159].
- [17] R. S. Raghavan, Talk given at the Int. Workshop on Neutrino Oscillations and their Origin (NOON2004), February 11 - 15, 2004, Tokyo, Japan; for further information see the web-site: <http://www.phys.vt.edu/~kimballton/> .
- [18] M. Nakahata, Talk given at the Int. Workshop on Neutrino Oscillations and their Origin (NOON2004), February 11 - 15, 2004, Tokyo, Japan.
- [19] Y. Suzuki, talk at Neutrino 2004, June 14-19 (2004), Paris, France; S. Schönert, talk at Neutrino 2002, Munich, Germany, (<http://neutrino2002.ph.tum.de>).
- [20] J. N. Bahcall and M. H. Pinsonneault, Phys. Rev. Lett. **92**, 121301 (2004) [arXiv:astro-ph/0402114].
- [21] A. Bandyopadhyay, S. Choubey, S. Goswami and K. Kar, Phys. Lett. B **519**, 83 (2001) [arXiv:hep-ph/0106264].
- [22] A. Bandyopadhyay, S. Choubey, S. Goswami and D. P. Roy, Phys. Lett. B **540**, 14 (2002) [arXiv:hep-ph/0204286]; S. Choubey, A. Bandyopadhyay, S. Goswami and D. P. Roy, arXiv:hep-ph/0209222.
- [23] A. Bandyopadhyay, S. Choubey, S. Goswami, S. T. Petcov and D. P. Roy, Phys. Lett. B **583**, 134 (2004) [arXiv:hep-ph/0309174].
- [24] A. Bandyopadhyay, S. Choubey, R. Gandhi, S. Goswami and D. P. Roy, J. Phys. G **29**, 2465 (2003) [arXiv:hep-ph/0211266]. A. Bandyopadhyay, S. Choubey, R. Gandhi, S. Goswami and D. P. Roy, Phys. Lett. B **559**, 121 (2003) [arXiv:hep-ph/0212146].

[25] Kevin Graham, talk at NOON 2004, February 11-15, 2004, Tokyo, Japan, <http://www-sk.icrr.u-tokyo.ac.jp/noon2004/>; H. Robertson for the SNO Collaboration, Talk given at TAUP 2003, Univ. of Washington, Seattle, Washington, September 5 - 9, 2003, <http://mocha.phys.washington.edu/taup2003>

[26] G.L. Fogli and E. Lisi, *Astropart. Phys.* **3**, 185 (1995).

[27] M. Apollonio *et al.* [CHOOZ Collaboration], *Phys. Lett. B* **466**, 415 (1999) [arXiv:hep-ex/9907037] ; M. Apollonio *et al.* [CHOOZ Collaboration], *Phys. Lett. B* **420**, 397 (1998) [arXiv:hep-ex/9711002]; M. Apollonio *et al.*, *Eur. Phys. J. C* **27**, 331 (2003) [arXiv:hep-ex/0301017]. F. Boehm *et al.*, *Phys. Rev. D* **64**, 112001 (2001) [arXiv:hep-ex/0107009].

[28] S.T. Petcov, *Phys. Lett. B* **214**, 259 (1988).

[29] S.T. Petcov, *Phys. Lett. B* **200**, 373 (1988), and *Phys. Lett. B* **214**, 139 (1988); S.T. Petcov and J. Rich, *Phys. Lett. B* **224**, 401 (1989); P.I. Krastev and S.T. Petcov, *Phys. Lett. B* **207**, 64 (1988); E. Lisi *et al.*, *Phys. Rev. D* **63**, 093002 (2000).

[30] A. Bandyopadhyay, S. Choubey, S. Goswami and K. Kar, *Phys. Rev. D* **65**, 073031 (2002) [arXiv:hep-ph/0110307];

[31] S. Choubey, S. T. Petcov and M. Piai, *Phys. Rev. D* **68**, 113006 (2003) [arXiv:hep-ph/0306017].

[32] S. Choubey and S. T. Petcov, *Phys. Lett. B* **594**, 333 (2004) [arXiv:hep-ph/0404103].

[33] J. F. Beacom and M. R. Vagins, arXiv:hep-ph/0309300.

[34] G. Eder, *Nucl. Phys.* **78**, 657 (1966).

[35] G. L. Fogli, E. Lisi, A. Palazzo and A. M. Rotunno, arXiv:hep-ph/0405139.

[36] G. Fiorentini, M. Lissia, F. Mantovani and R. Vannucci, arXiv:hep-ph/0409152. F. Mantovani, L. Carmignani, G. Fiorentini and M. Lissia, *Phys. Rev. D* **69**, 013001 (2004) [arXiv:hep-ph/0309013]. G. Fiorentini, T. Lasserre, M. Lissia, B. Ricci and S. Schonert, *Phys. Lett. B* **558**, 15 (2003) [arXiv:hep-ph/0301042]. H. Nunokawa, W. J. C. Teves and R. Zukanovich Funchal, *JHEP* **0311**, 020 (2003) [arXiv:hep-ph/0308175].

[37] H. Minakata, H. Nunokawa, W. J. C. Teves and R. Zukanovich Funchal, arXiv:hep-ph/0407326.